united nations
educational, scientific
and cultural
organization

international atomic
energy agency

the
abdus salam
international centre for theoretical physics

ICTP 40th Anniversary

SCHOOL ON SYNCHROTRON RADIATION AND APPLICATIONS
In memory of J.C. Fuggle & L. Fonda

19 April - 21 May 2004

Miramare - Trieste, Italy

1561/40

Contrast mechanisms and detectors used in full-field imaging and scanning transmission x-ray microscopes

B. Kaulich

Contrast mechanisms and detectors used in full-field imaging and scanning transmission x-ray microscopes

Burkhard Kaulich

Sincrotrone Trieste, X-ray Microscopy Section

Aim of the lecture

This lecture aims at introducing different contrast and detector technologies

and giving a comparison between techniques used for visible light and X-rays

Structure of the lecture

- Necessary background information
- Basic principles of contrast techniques
- Introduction to visible light techniques
- Comparison of visible light techniques with X-ray techniques
- Detector technologies
- Influence of detector principles to imaging contrast

Background info: X-ray microscopy types

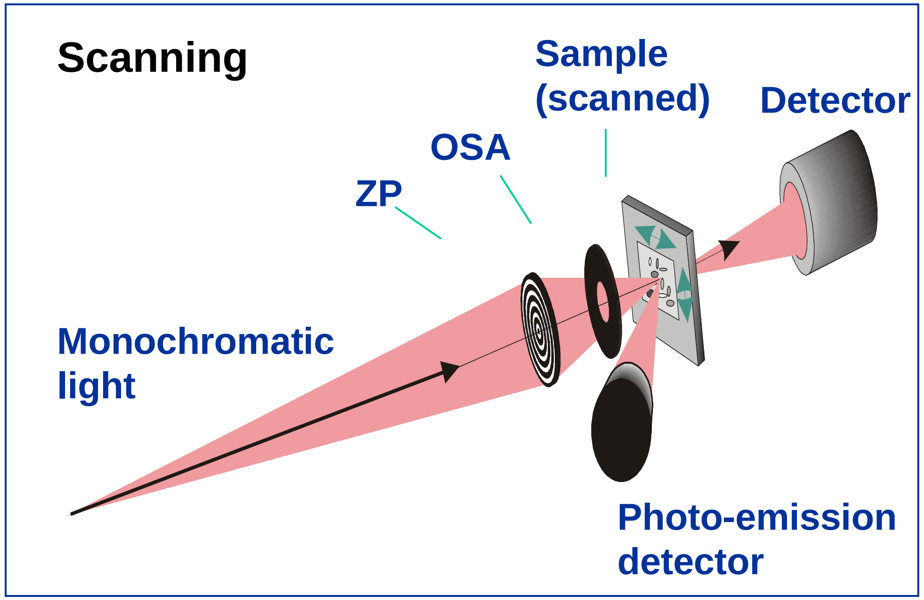

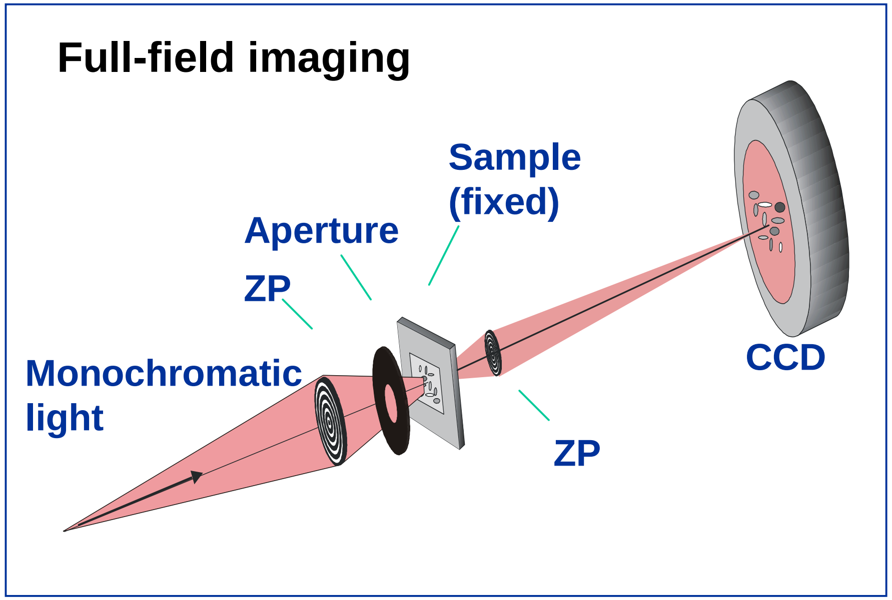

+ versatile detectors can run simultaneously;
+ easier optics set-up;
- long exposure time;
- complex electronics.

Ideal for spectromicroscopy

+ short exposure time;
+ higher resolution - static system;
- complex optical alignment.

Ideal for dynamic studies and tomography

Background info: Zone plates

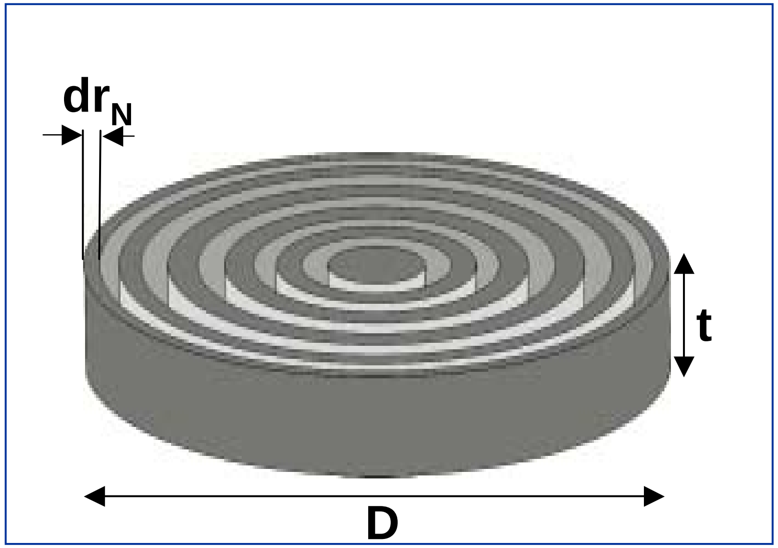

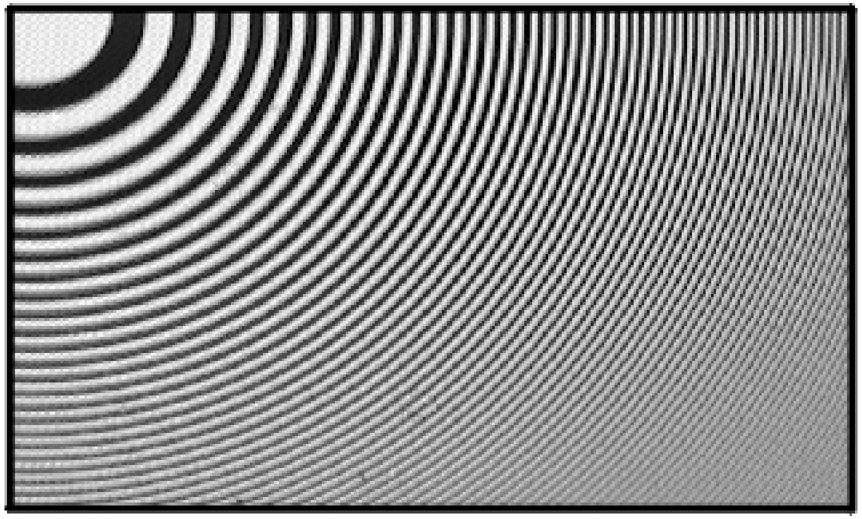

Zone plate is a circular diffraction grating with radially decreasing line width

$$\frac{1}{f} = \frac{1}{p} + \frac{1}{q} \quad \text{if} \quad n > 100$$

In terms of ZP parameters:

$$f_m = \frac{2}{m} D\, dr_N / \lambda$$

To avoid chromatic aberrations:

$$\frac{E}{\Delta E} \geqq n\, m$$

Background info: Spatial resolution of ZPs

$$\delta = \sqrt{(1.22\Delta r_N)^2 + \left(\sigma\frac{q}{p}\right)^2 + \left(\varnothing\frac{\Delta E}{E}\right)^2}$$

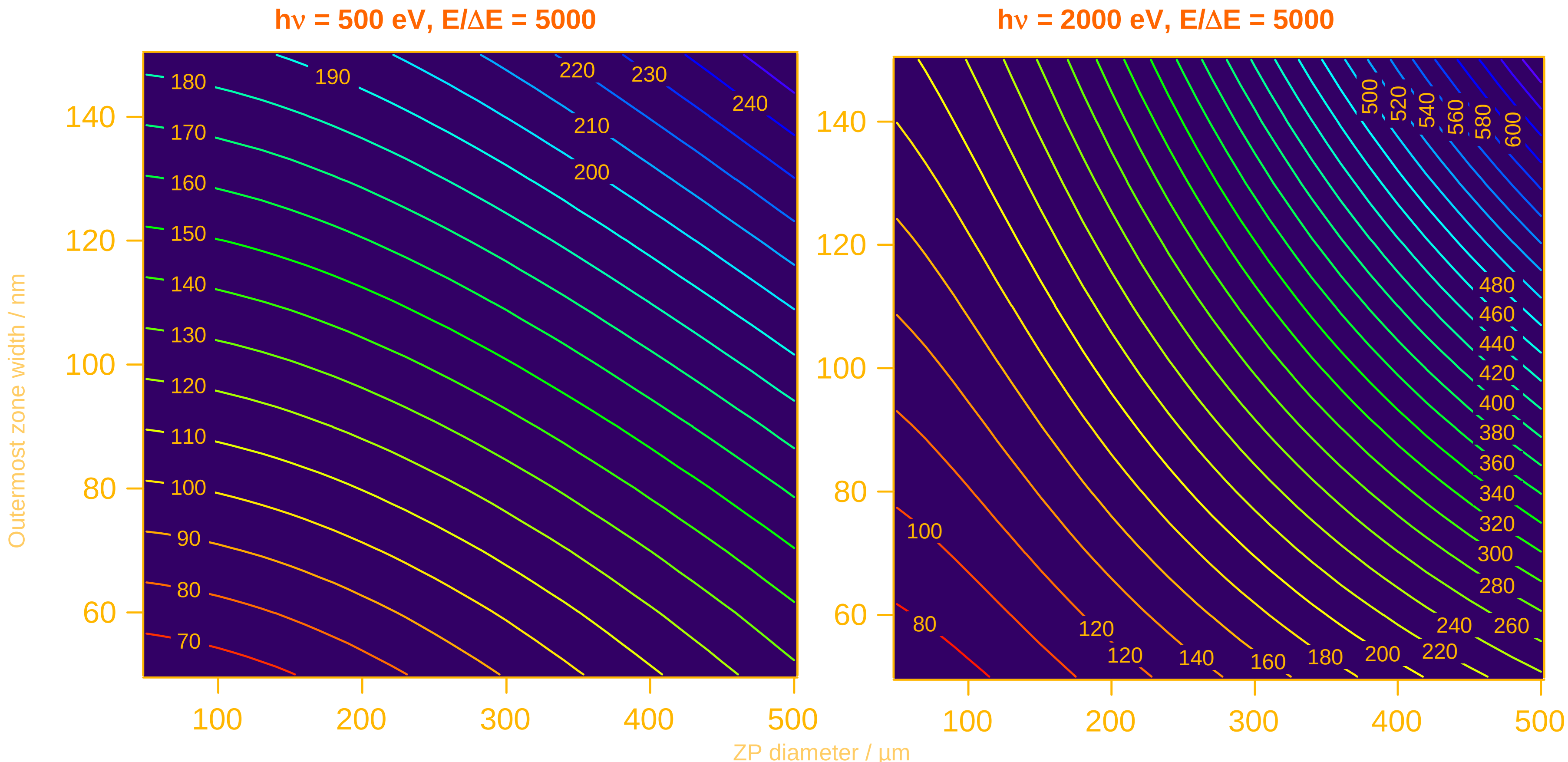

Refractive index and contrast for X-rays

Refractive index n(λ):

$$n(\lambda) = 1 - \delta(\lambda) - i\beta(\lambda) = 1 - \frac{n_a r_e \lambda^2}{2\pi} f_1(\lambda) - f_2(\lambda)$$

δ(λ): Phase term
β(λ): Absorption term
n_a: average atom density
r_e: classical electron radius
f_1, f_2: atomic form factors

- **Refractive index *n* is close to unity**
- **Refractive index *n* is slightly smaller than unity**
- **Ratio δ/β can be considerably large**
- **f1, f2 tabulated by *Henke et al.***

Refractive index and X-ray contrast techniques

X-ray contrast is generated by *differences* in the complex scattering factor per unit volume

$$\delta(\lambda) = \frac{n_a r_e \lambda^2}{2\pi} f_1(\lambda)$$

$$\beta(\lambda) = \frac{n_a r_e \lambda^2}{2\pi} f_2(\lambda)$$

⇩

Absorption:

- Bright-field imaging
- Chemical contrast techniques
- Magnetic contrast techniques

⇩

Scattering, refraction:

- Zernike phase contrast
- Differential phase contrast
- Differential interference contrast
- Dark-field imaging

Basic principles of contrasts

- Contrast is not an inherent property of the specimen, but is dependent upon interaction of the specimen with light AND the efficiency of the optical system to record the image to the detector

- Human eye needs at least about 2% image contrast to distinguish between image and background

- Values might vary for other detectors

- With each detector, the signal to noise ratio must be large enough to be interpreted in terms of the formation of an image

Definition of contrast

Often applied definition:

Contrast is defined as the difference in light intensity between the image and the adjacent background relative to the overall background intensity

$$C = 100 \cdot \frac{(I_S - I_B)}{I_B}$$

I_s: Specimen intensity
I_b: Background intensity

Definition used for XRM:

Contrast is defined as the difference in maximum and minimum light intensity normalized to the sum of maximum and minimum light intensity

$$C = \frac{(I_{\max} - I_{\min})}{I_{\max} + I_{\min}}$$

I_{max}: Max. image intensity
I_{min}: Min. image intensity

Natural amplitude contrast between water and organic matter

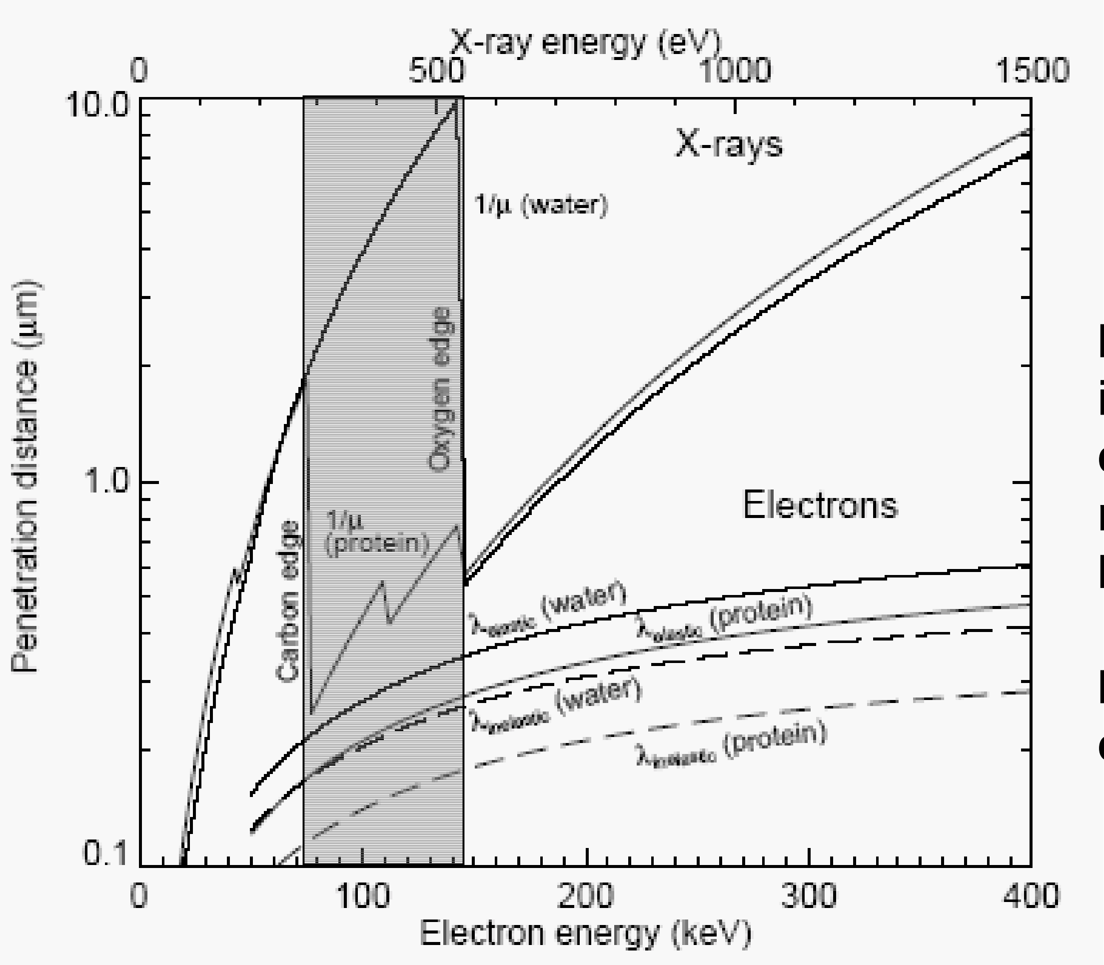

<u>The “Water Window”:</u>

283 eV < hν < 532 eV

Due to dramatic difference in the f2 values of two materials, especially water and organic matter between the C and O K-absorption edges.

Note the penetration distance compared to electrons !!!

H. Wolter: *Spiegelsysteme streifenden Einfalls als abbildende Optiken fuer Roentgenstrahlen*, Ann. Phys. **10**, 94-114, 286 (1952)

Brightfield imaging in the “water window”

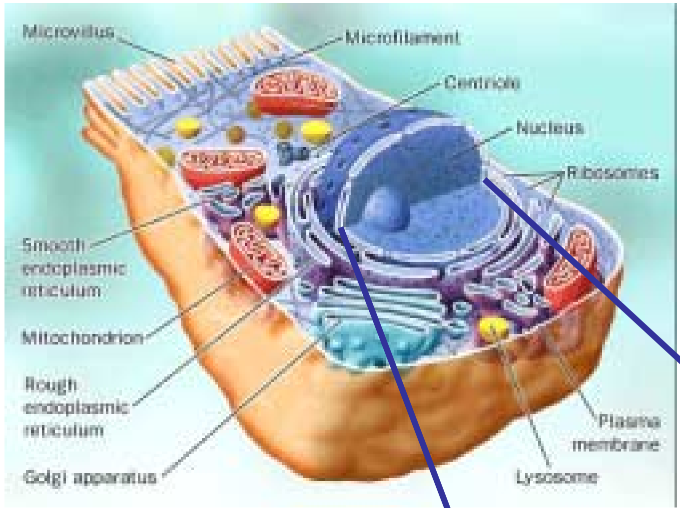

Location of Splicing Factors in whole, hydrated human mammary epithelial cells (ALS, TXM XM1)

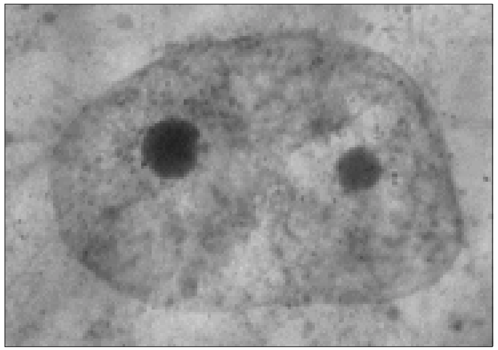

Control nucleus, no primary antibody

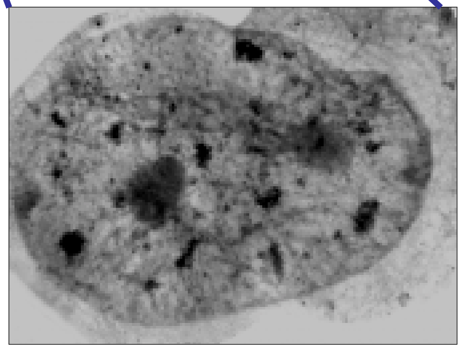

Single nucleus labeled using antibodies specific for splicing factors

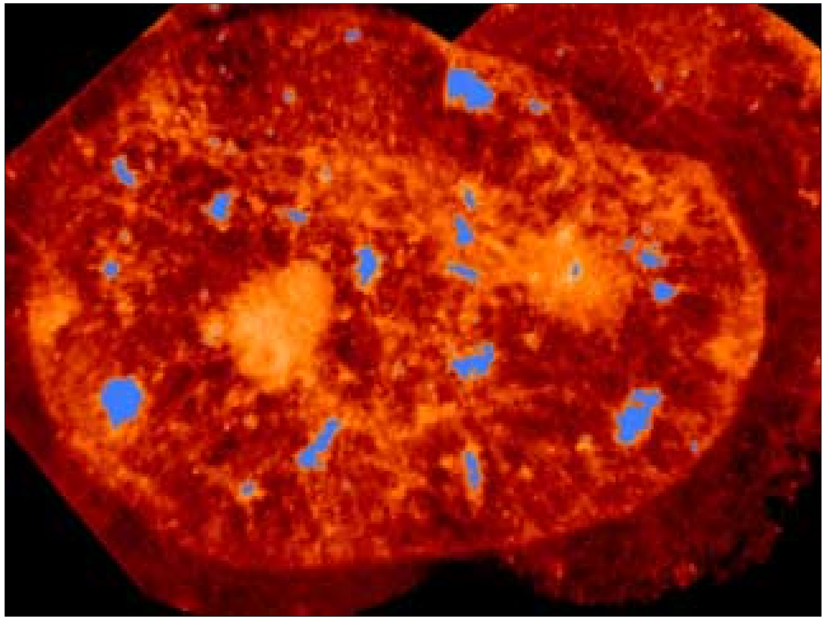

Same nucleus, splicing factors colored blue

C. Larabell et al., Live Science Division, LBL, USA

Water window brightfield imaging in combination with tomography

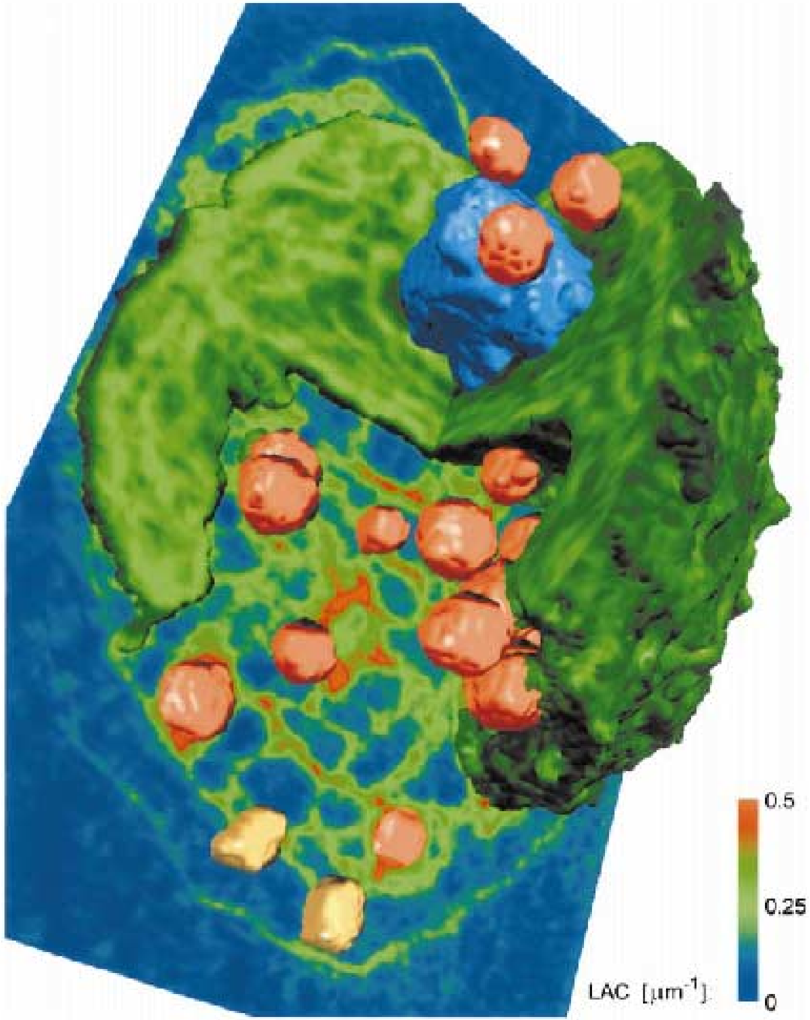

X-ray tomography of hydrated specimen "close to their living state"

Alga: Chlamydomonas reinhardtii

Acquired with the full-field imaging Microscope at BESSY I

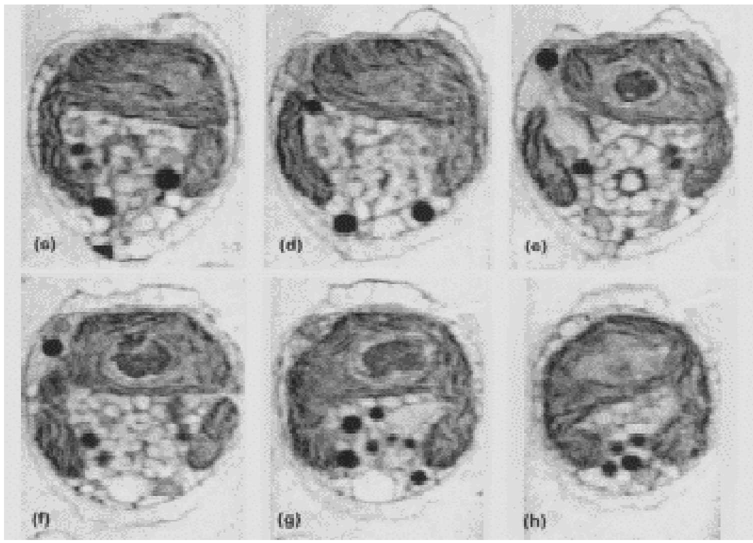

D. Weiss et al., University of Goettingen

Brightfield imaging at higher photon energies

Characterization of morphology and defects in modern semiconductors with a full-field imaging microscope (@ 1.8 keV, XM1/ ALS)

Sample preparation:
Back side thinning of Si wafer

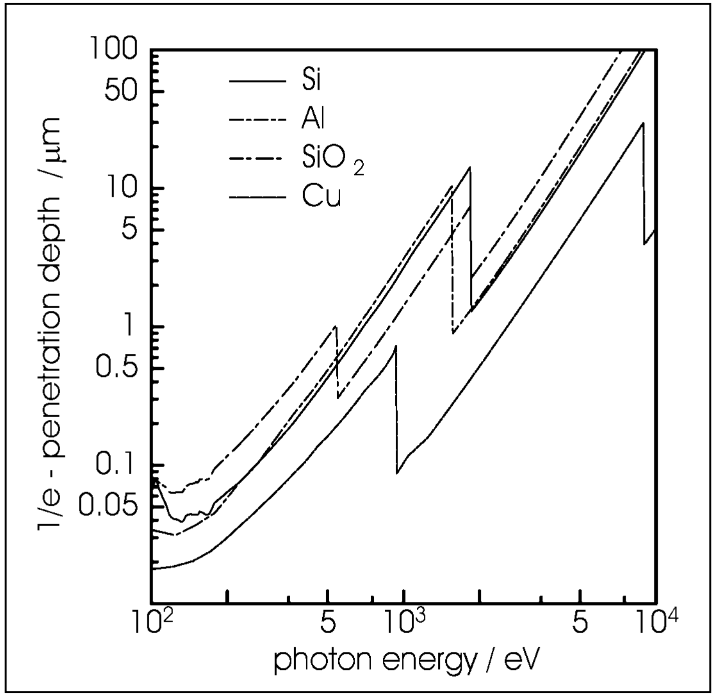

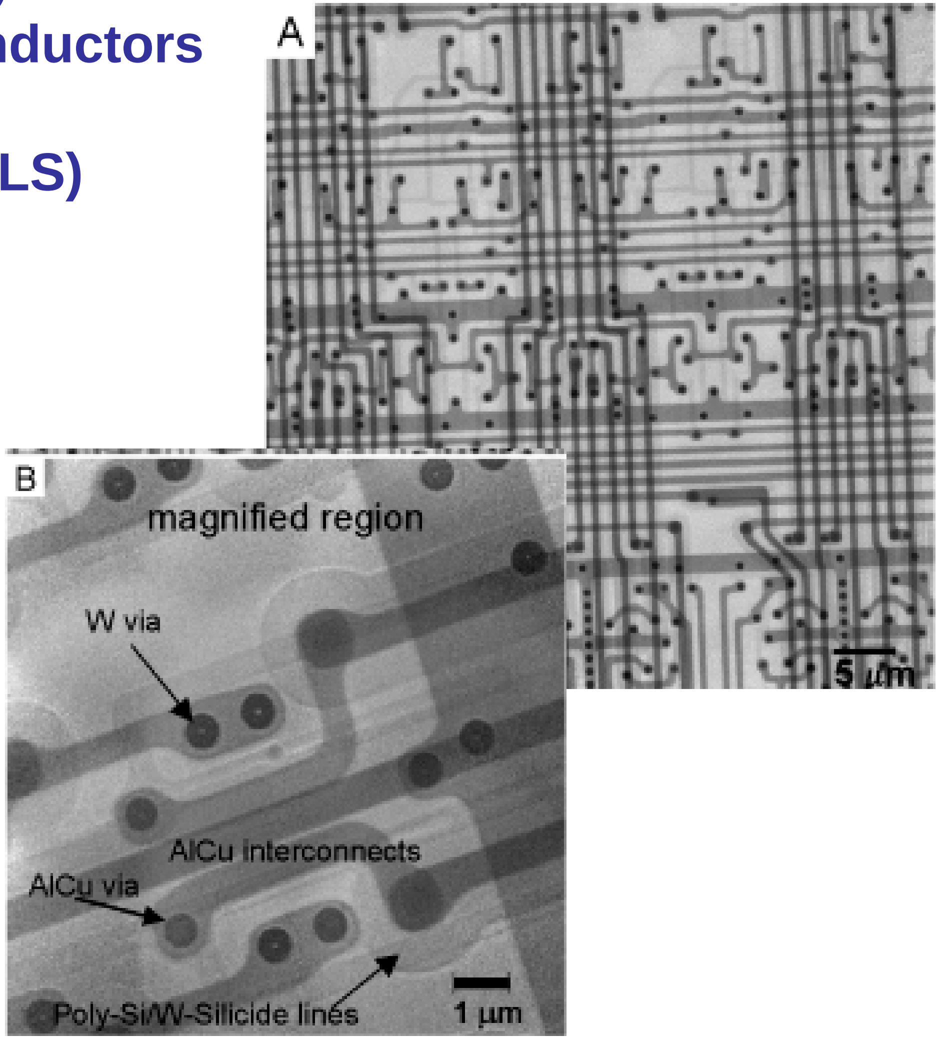

G. Schneider et al., BESSY II

Darkfield imaging

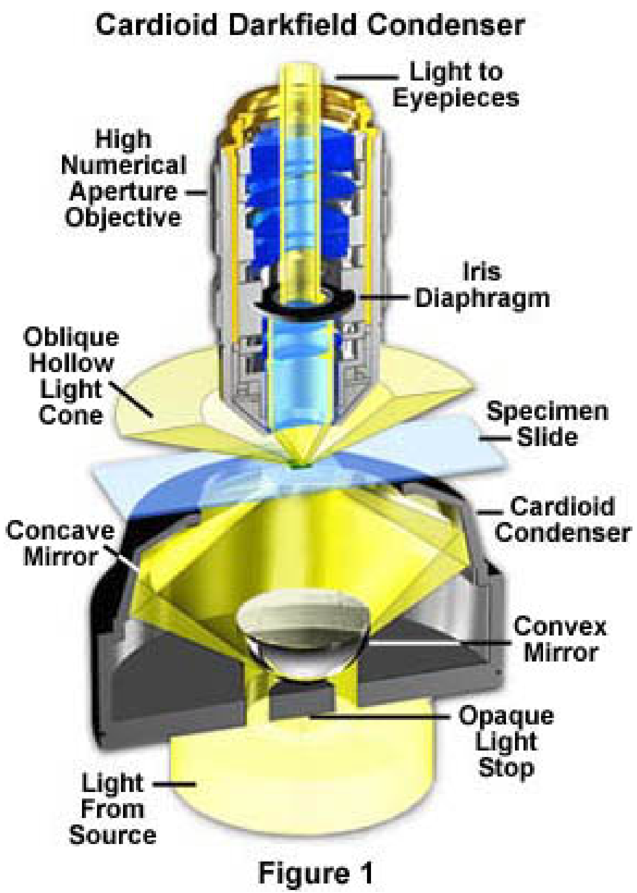

Darkfield imaging in X-ray microscopy

Basics: Zernike phase contrast

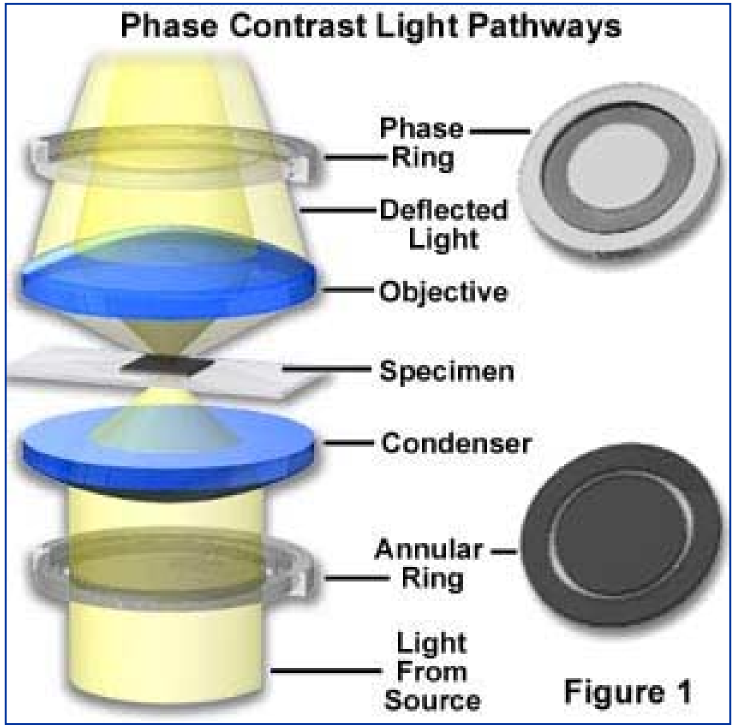

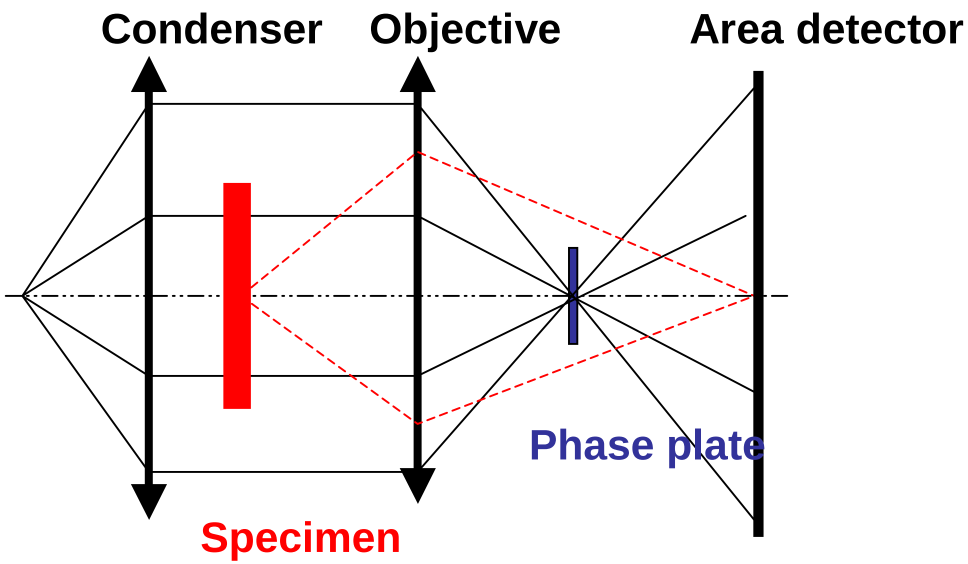

$$A_{specimen} = A_{surr} e^{i\Phi} = A_{surr} e^{i\frac{2\pi}{\lambda}\Delta t} \approx A_{surr}(1 + i\Phi) \qquad \Phi << 1$$

Phase plate in "back-focal" plane: Phase of A_{surr} can be shifted by +/- $\pi/2$!!!

Phase differences are converted in amplitude differences !!!

Zernike phase contrast in full-field imaging X-ray microscopy

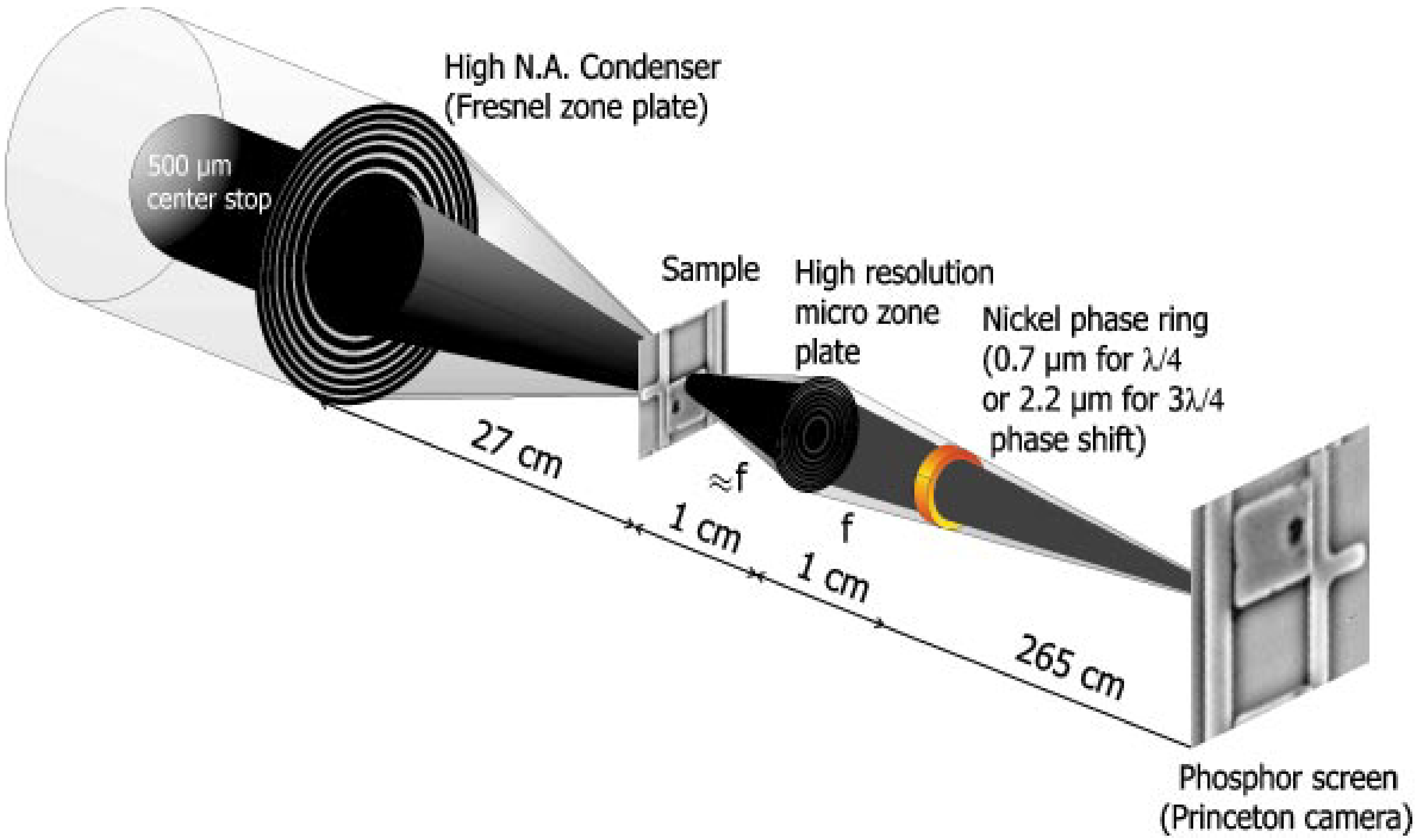

Zernike phase contrast in X-ray microscopy

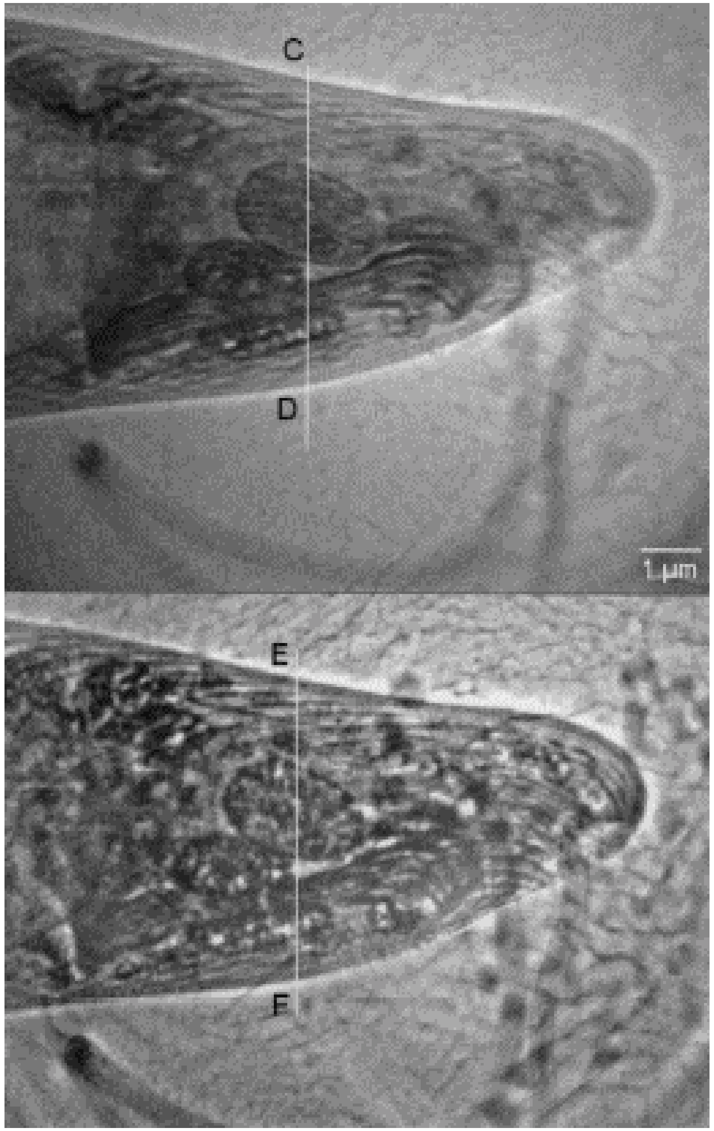

Amplitude and Zernike phase contrast images of an alga *Euglena gracilis*

E = 500 eV, accumulated dose is $3x10^6$ Gray

Amplitude: 3 s
Phase contrast: 15 s

Drawbacks of Zernike phase contrast:

- **Halos around structures**
- **Quantitative analysis difficult**
- **Limitation in spatial resolution**
- **Not all spatial frequencies are treated equally**

Principle of Differential interference contrast

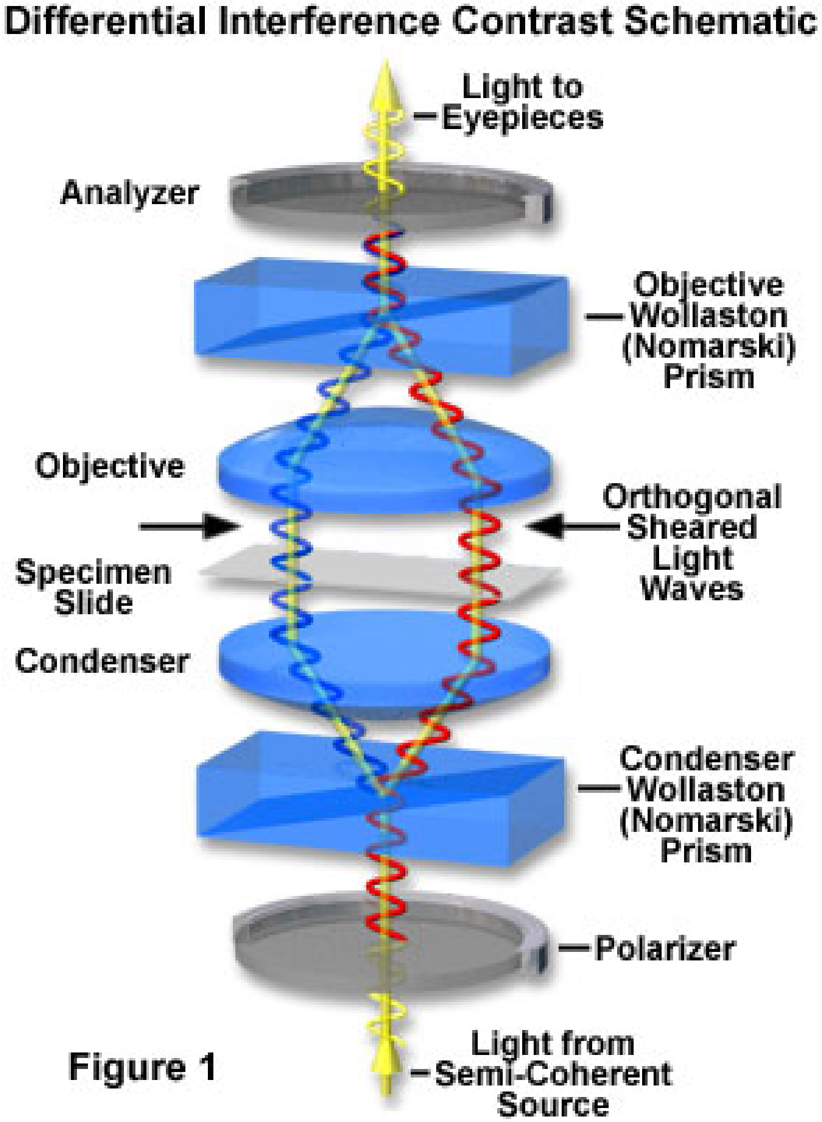

- Light is polarized beneath the condenser optic
- Light pass is split by a modified Wollaston prism
- Sheared waves are recombined by a "Nomarski" prism

Difficulty for X-rays:

No way to create prisms necessary for beam shearing

Crystal shearers are too large to be implemented in the optical scheme and not appropriate for soft X-rays

Diffractive optics interferometry with X-rays

Principle: ***Wave front division by different diffraction orders of zone zone plate(s)***

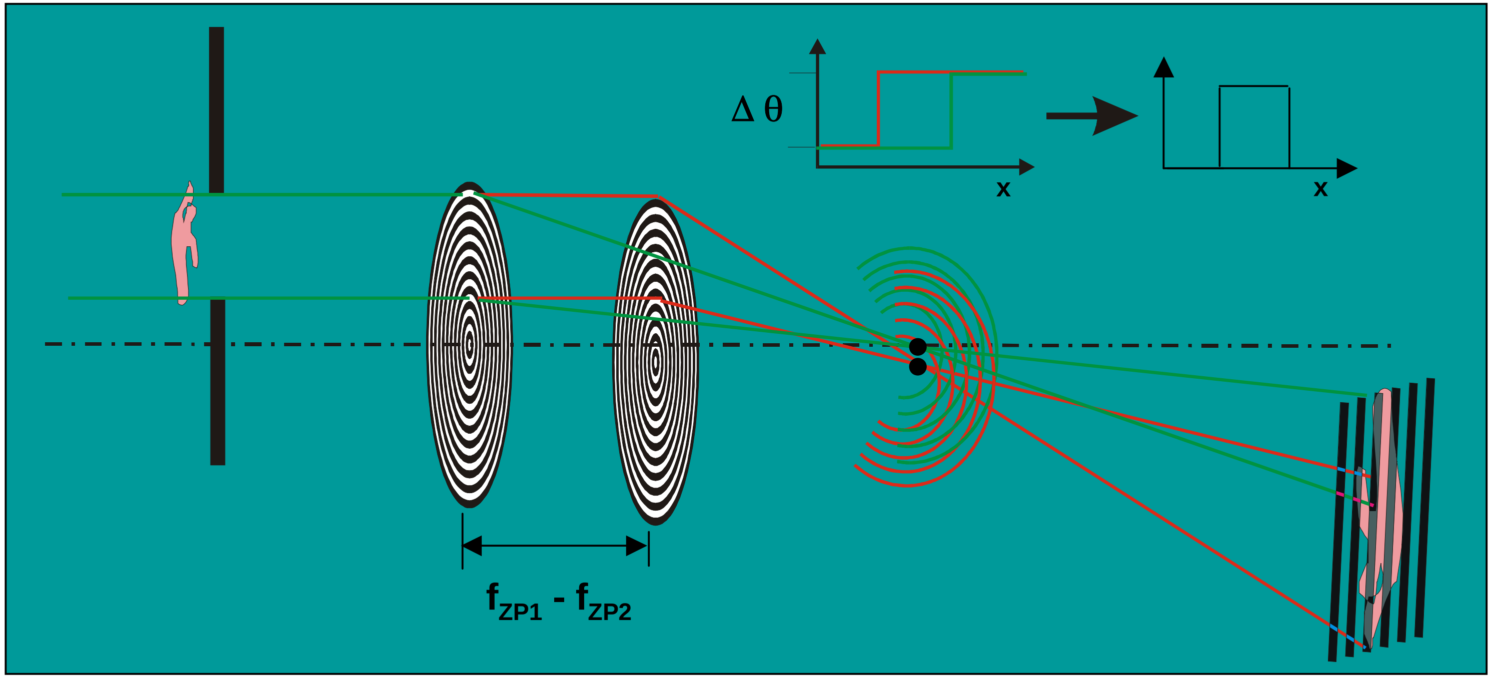

- **Wave front division with as small as possible shears possible**
- **Interference pattern is overlapped to a X-ray image**

Diffractive optics interferometry with X-rays

Control of the interference pattern

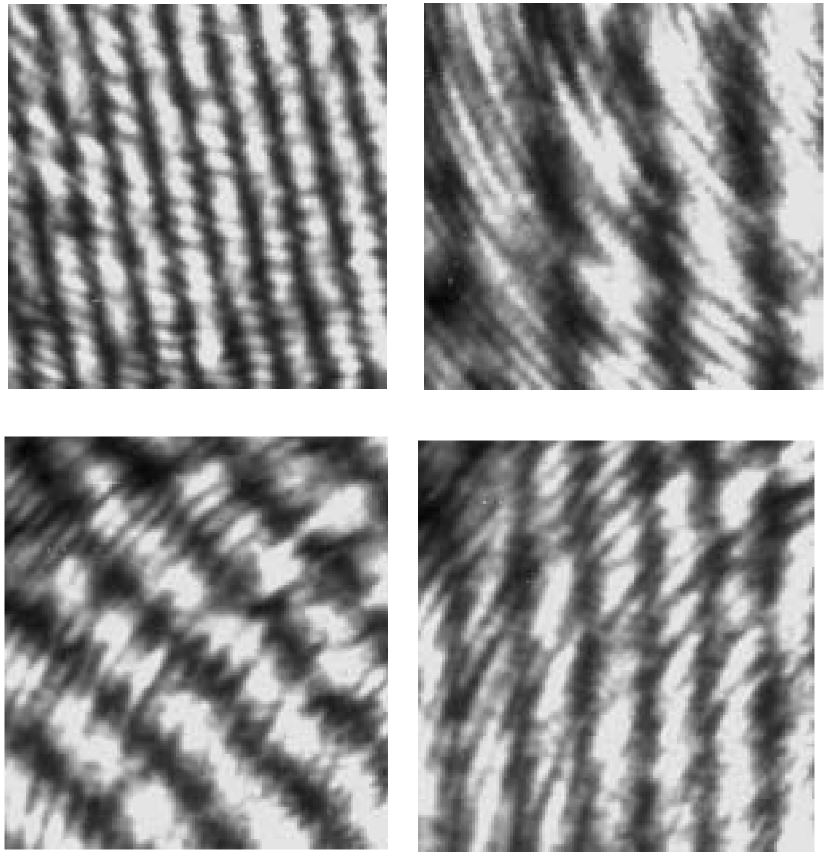

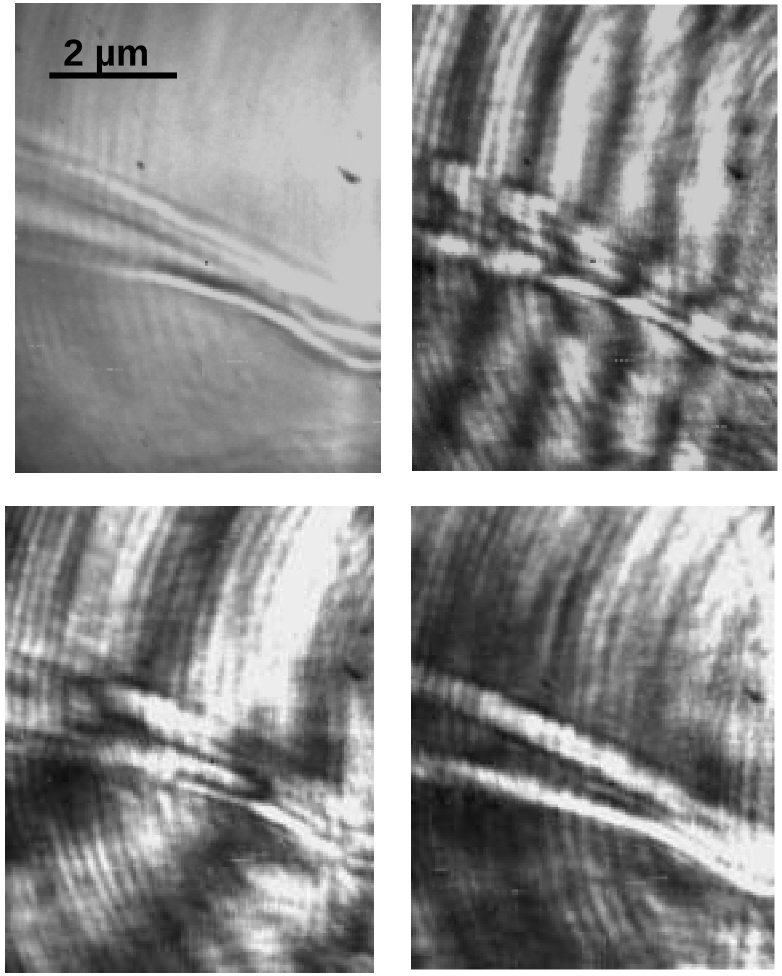

Edge of 50 µm Kapton foil

T. Wilhein, B. Kaulich, J. Susini (accepted for Opt. Communic.)

The principle of X-ray DIC in detail

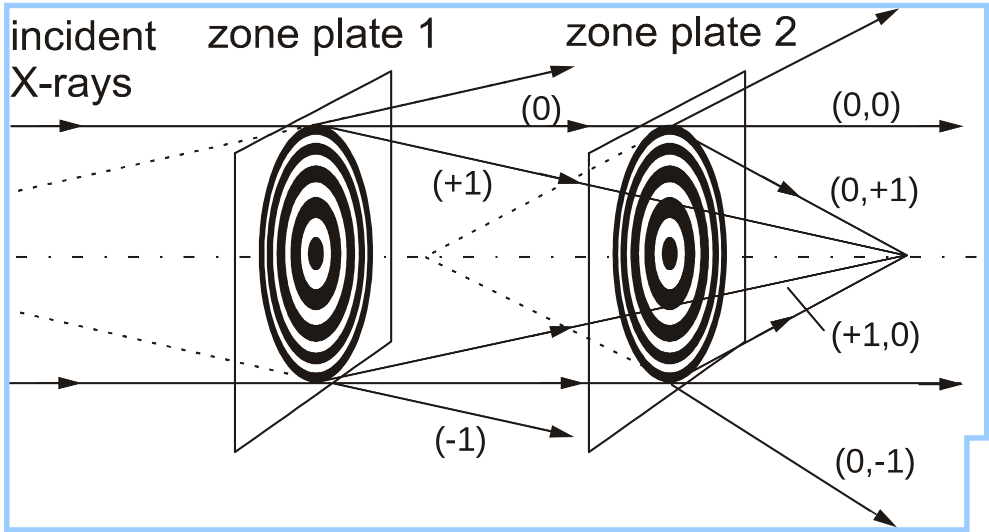

Two zone plates split and combine an incident wave in a set of waves that may interfere behind zone plate 2.

Two zone plates with focal length f_1 and f_2 separated by f_1-f_2 allow for best fringe control (only relevant beams displayed).

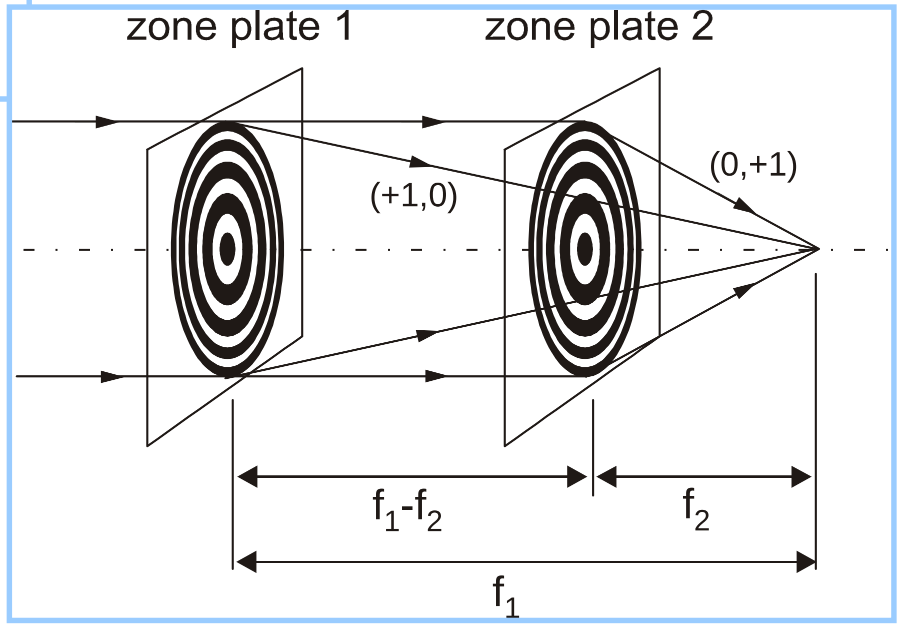

Coherence considerations for DIC with X-rays

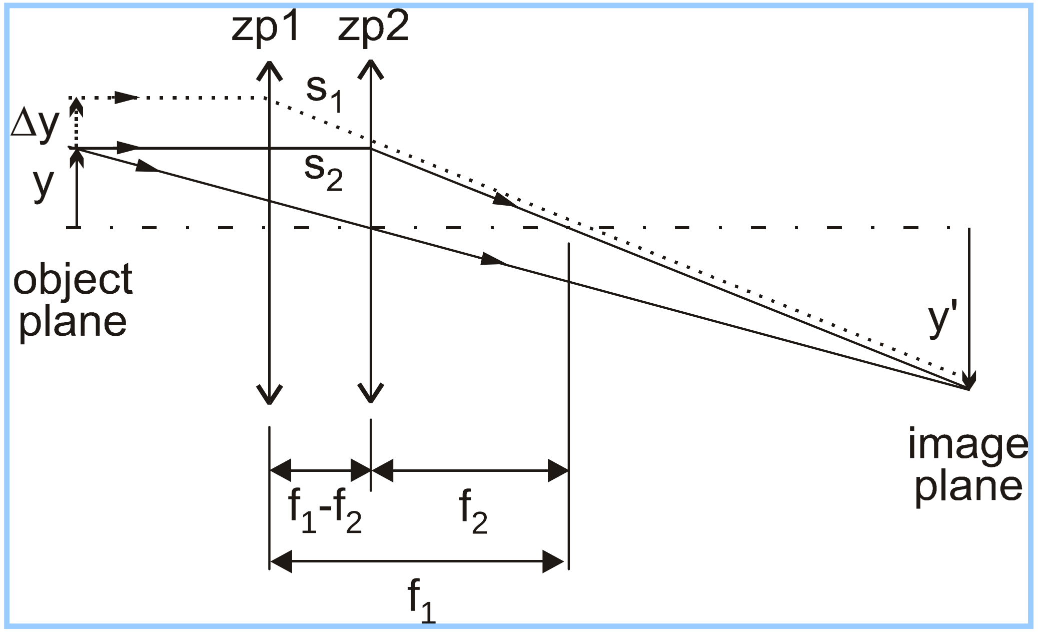

Temporal coherence

$$\Delta s \approx \frac{\Delta y^2}{2\cdot(f_1 - f_2)} = \frac{(f_1 - f_2)\cdot y^2}{2\cdot f_2{}^2}$$

$\Delta s <$ coherence length l_{coh}

Spatial coherence

$$\Delta y = \frac{\left(f_1 - f_2\right)}{f_2}\cdot y$$

$\Delta y <$ coherently illuminated field D

Spatial coherence considerations for X-rays with DIC

ZP focal length and spatial resolution

$$f = 2\,r \cdot \Delta r / \lambda$$

$$\delta = 1.22 \cdot \Delta r$$

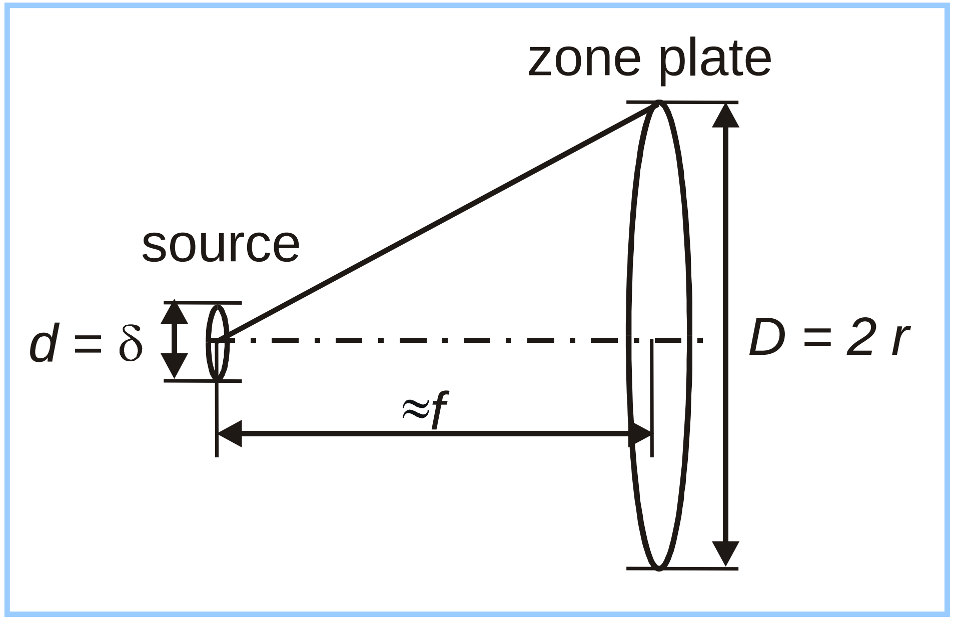

Coherently illuminated field (van Zittert - Zernike)

$$D = 0.61 \cdot \frac{L \cdot \lambda}{d/2} = 0.61 \cdot \frac{f \cdot \lambda}{\delta/2}$$

Result:

$$D = 0.61 \cdot \frac{f \cdot \lambda}{\delta/2} = 0.61 \cdot \frac{f \cdot \lambda}{1.22 \cdot \Delta r/2} = 0.61 \cdot \frac{f \cdot \lambda \cdot 2 \cdot r}{1.22 \cdot \lambda \cdot f/2} = 2 \cdot r$$

DIC intrinsically coherent !

Temporal coherence considerations for DIC with X-rays

Monochromaticity needed for zone plate imaging

$$\frac{\lambda}{\Delta\lambda} \geq N$$

Effective radius of ZPD

$$r_{eff} = r + a \approx r + \Delta r$$

Effective number of zones of ZPD

$$N_{eff} \approx \frac{(r + \Delta r)^2}{\lambda \cdot f} = N + 1 \approx N$$

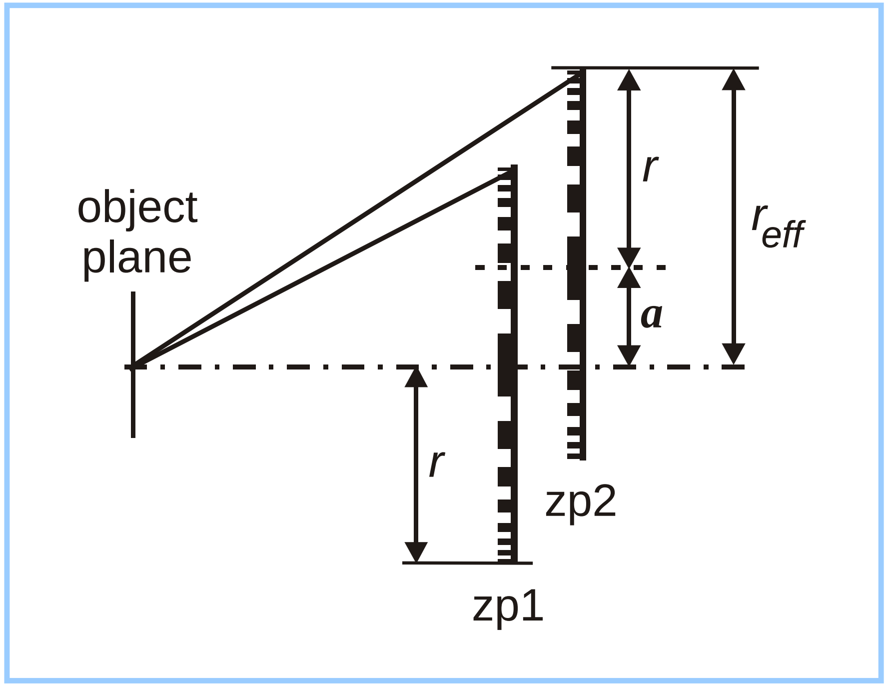

No constraints stronger than for single zone plates !

Optical setup for DIC with X-rays in the TXM mode

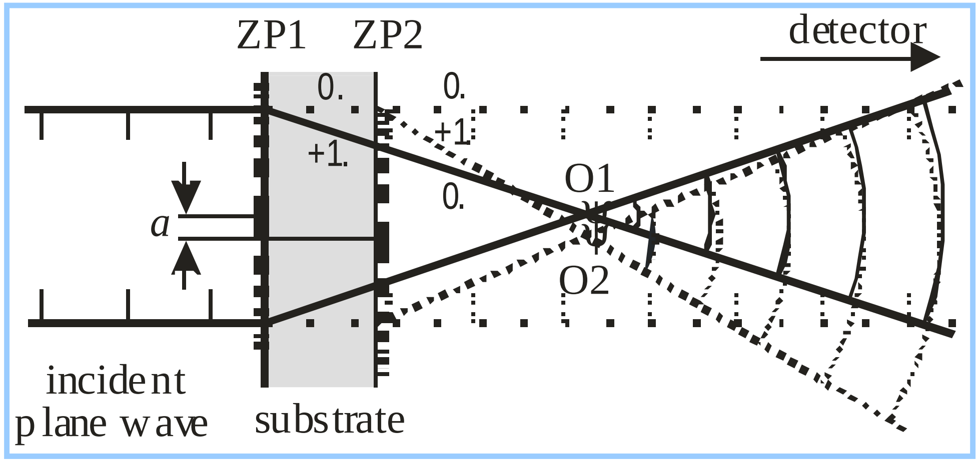

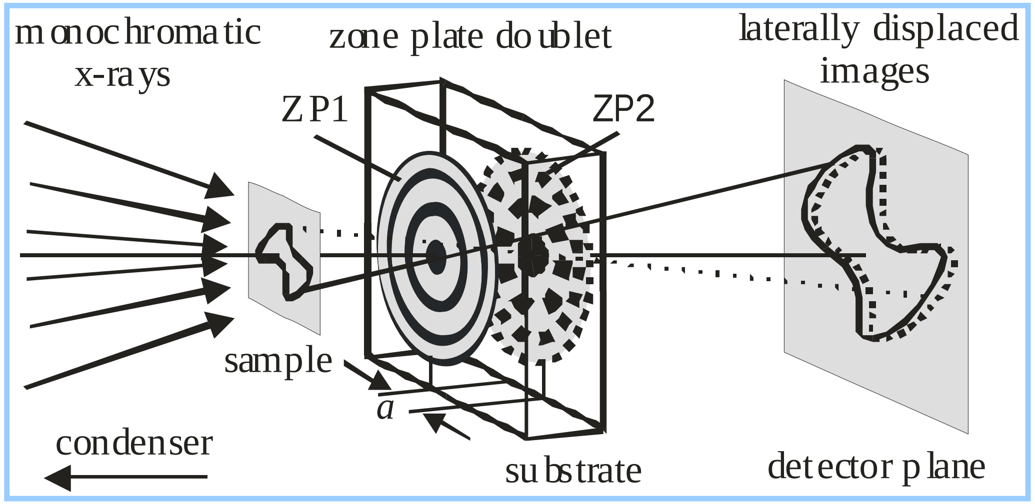

From an incident plane wave, the ZPD creates two spherical waves originating from O1 and O2 in its back focal plane

Fabrication of a “two ZP” setup

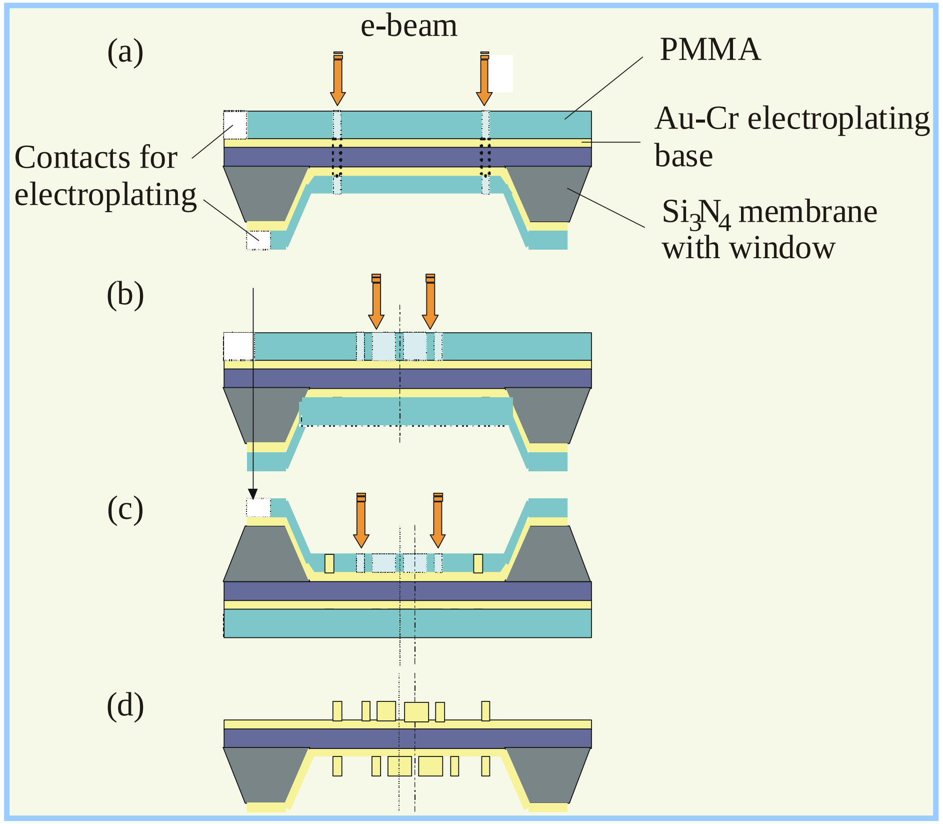

Generation process of ZPDs

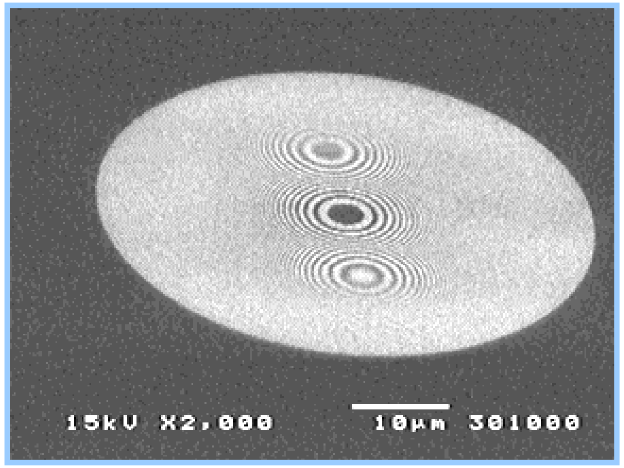

SEM micrograph

VIS microscope image

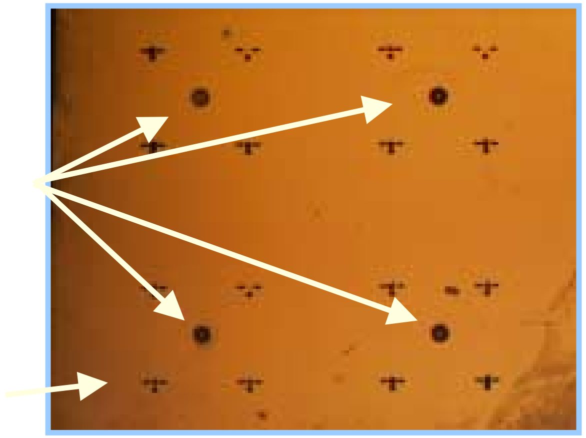

four ZPDs

registration marks

DIC with a full-field imaging microscope

X-ray microscope images of a 2 µm thick PMMA test object taken at ID21 at ESRF.

left side: bright field

right side: X-DIC with ZPD

λ = 0.31 nm

exposure time 20 s

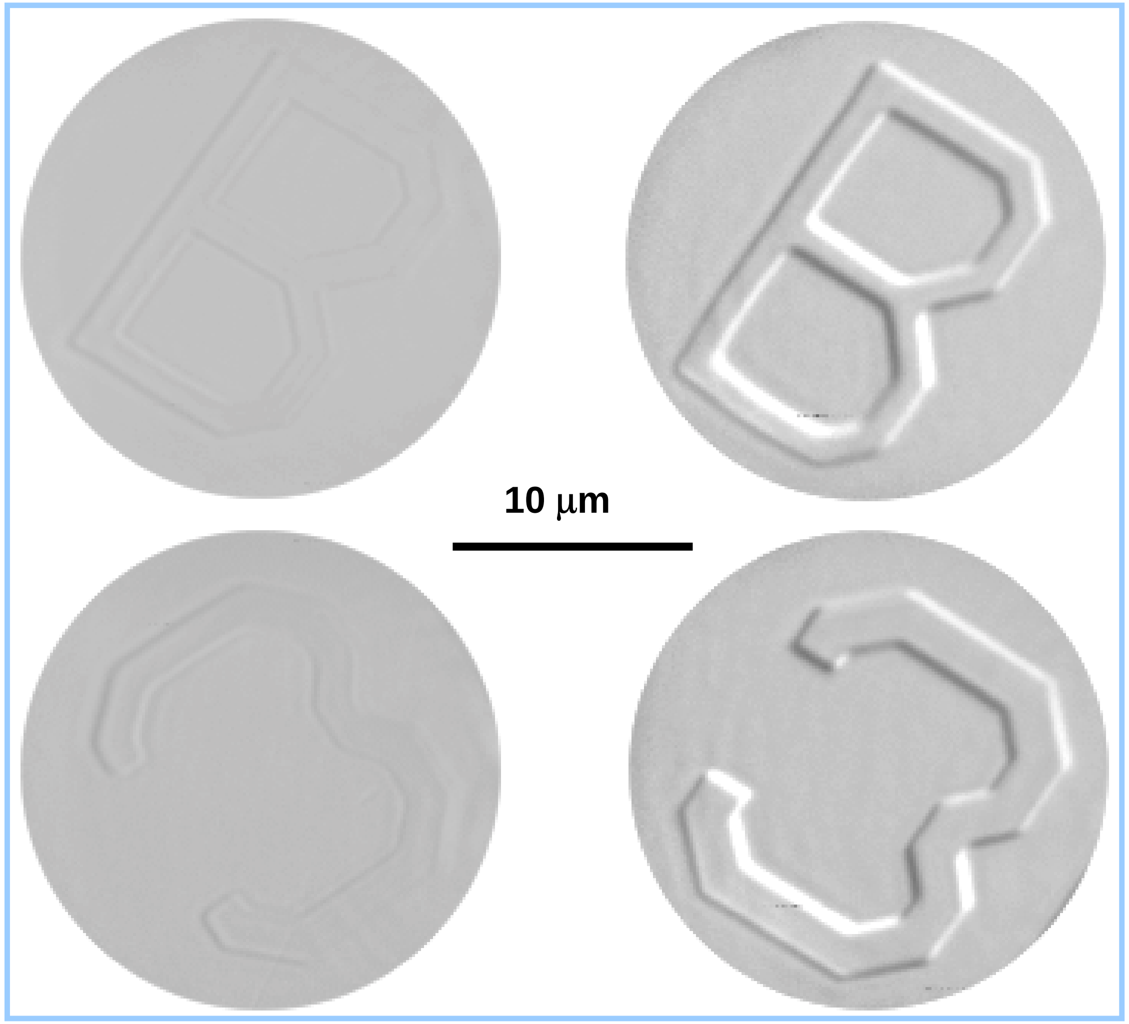

DIC with a full-field imaging setup

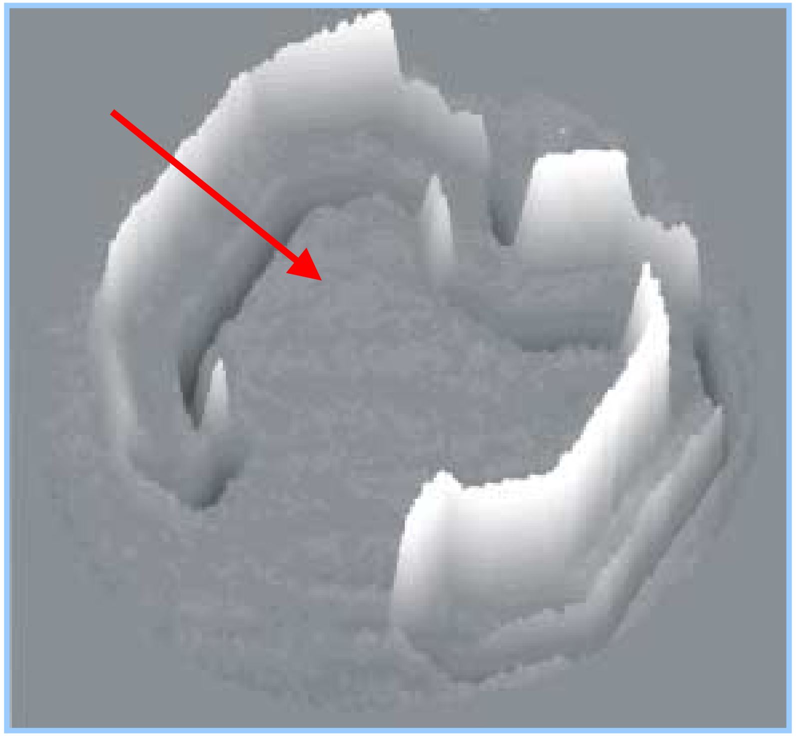

3d contour-plot of letter “ 3 “

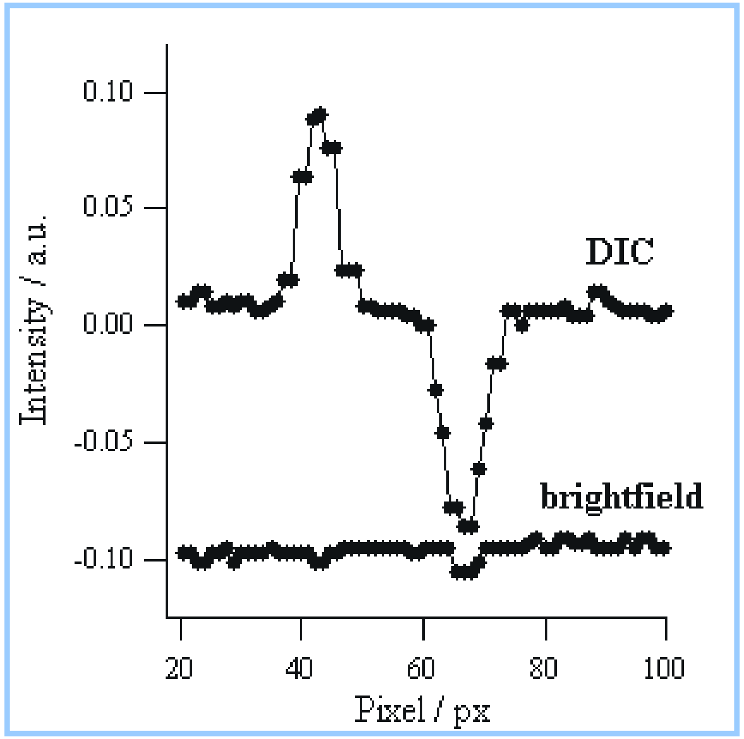

line scan across object feature

DIC with a scanning X-ray microscope

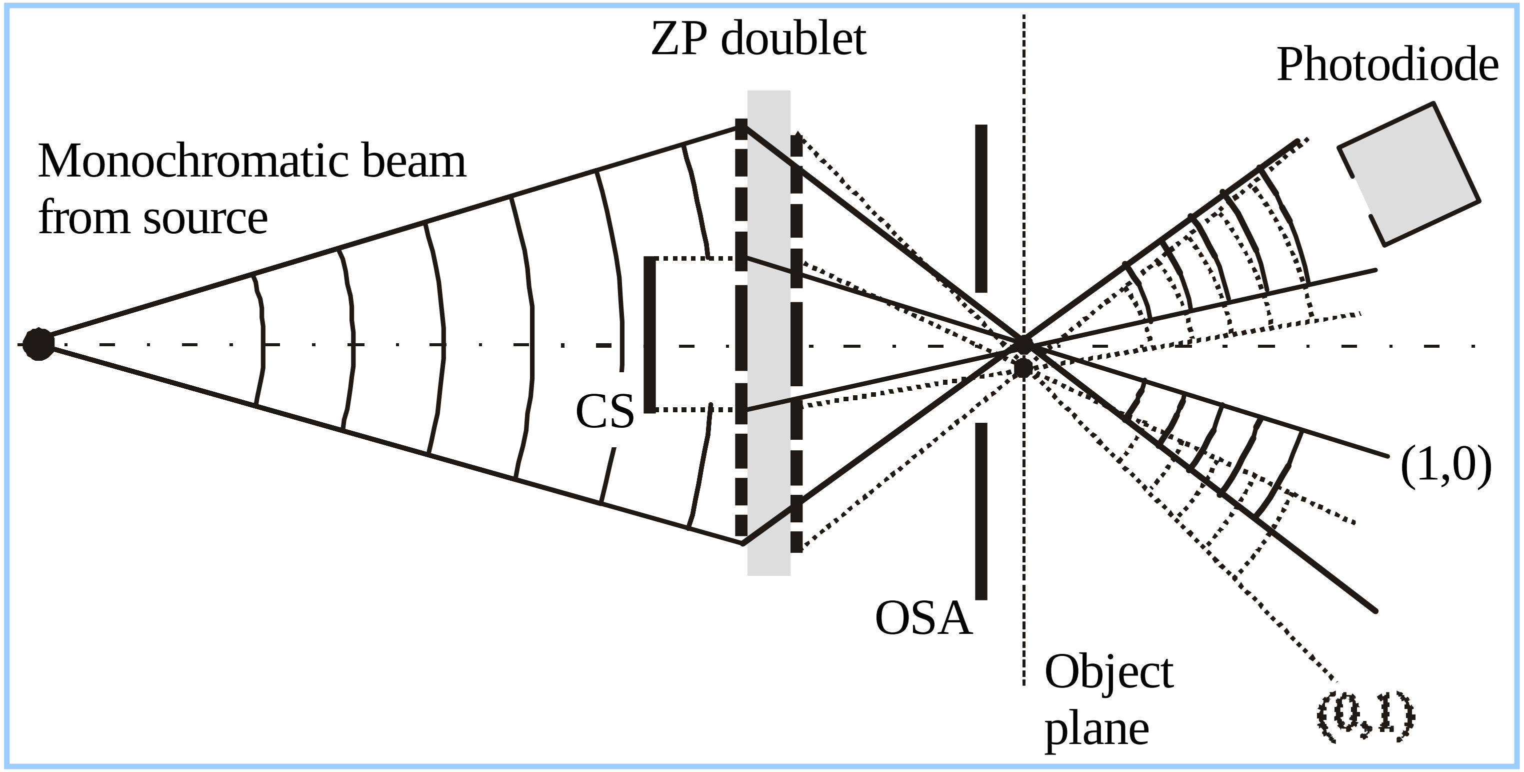

The ZPD creates two spots in the object plane. The phase shift between the two waves introduced by the object leads to interference contrast detected by the photodiode

DIC with a scanning X-ray microscope

Raster scan across +1. diffraction order with 50 µm aperture in front of photodiode

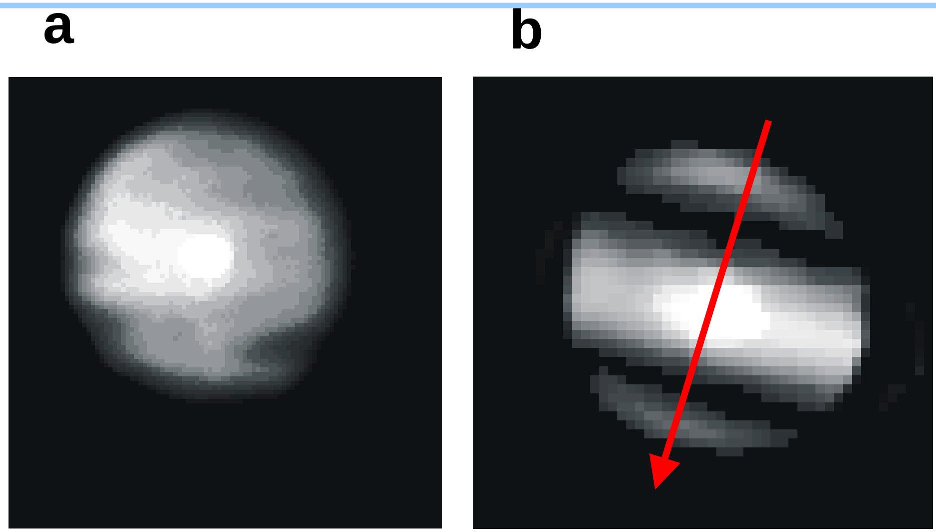

a: single ZP

b: ZPD generates interference pattern

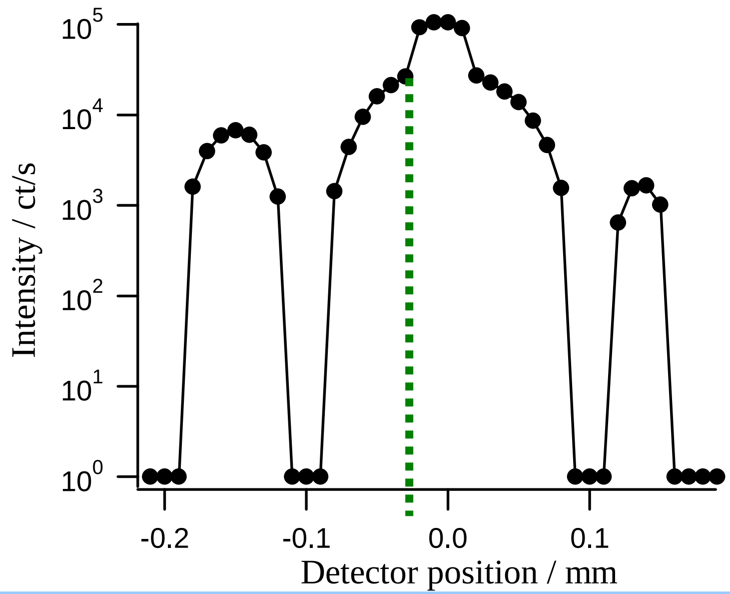

line scan across image b

DIC with a scanning X-ray microscope

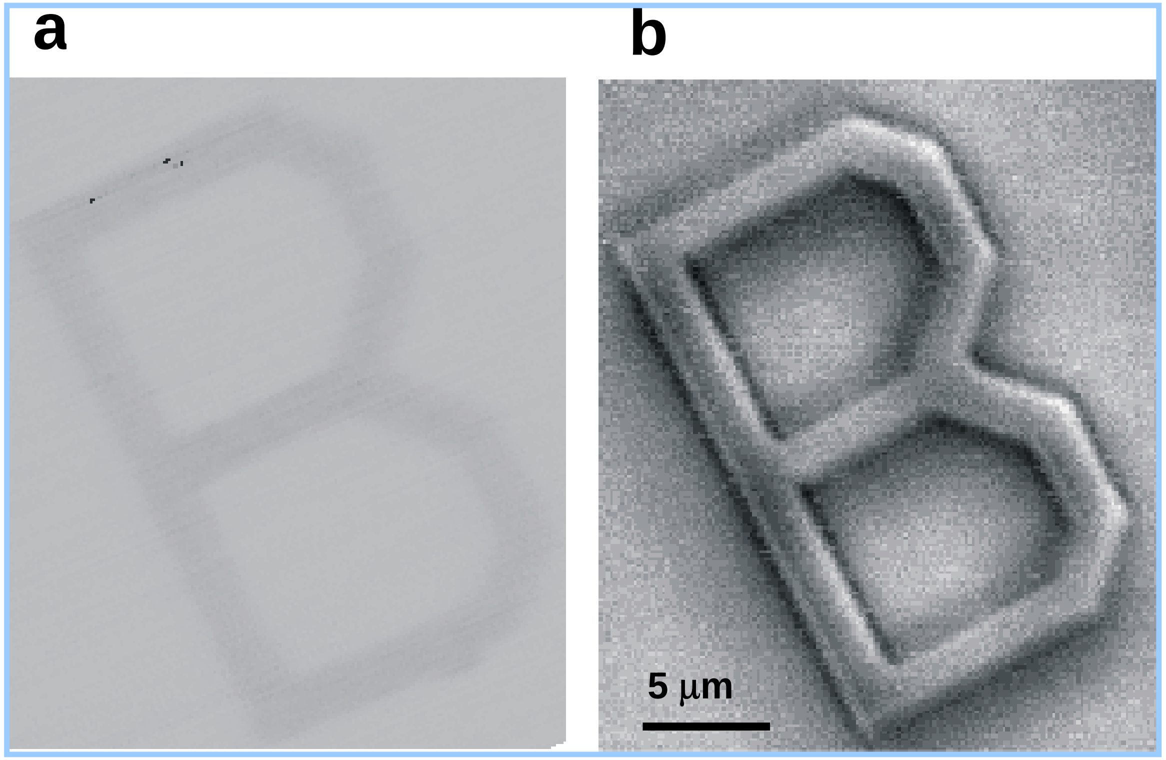

2 µm thick PMMA test object. Images taken with the STXM at ID21 at ESRF.

a: bright field

b: X-DIC with ZPD

pixel size 100 nm, field of view 20 µm

λ = 0.31 nm, dwell time 50 ms / pixel

Multi-spot ZPs for DIC

PDEs for X-DIC

a) two spots in focal plane,
   seperation 200 nm

b) four spots in focal plane,
   separation 200 nm

c) two spots along optical axis,
   separation 1 mm

f = 5 mm @ λ = 0.31 nm

calculated zone plate patterns

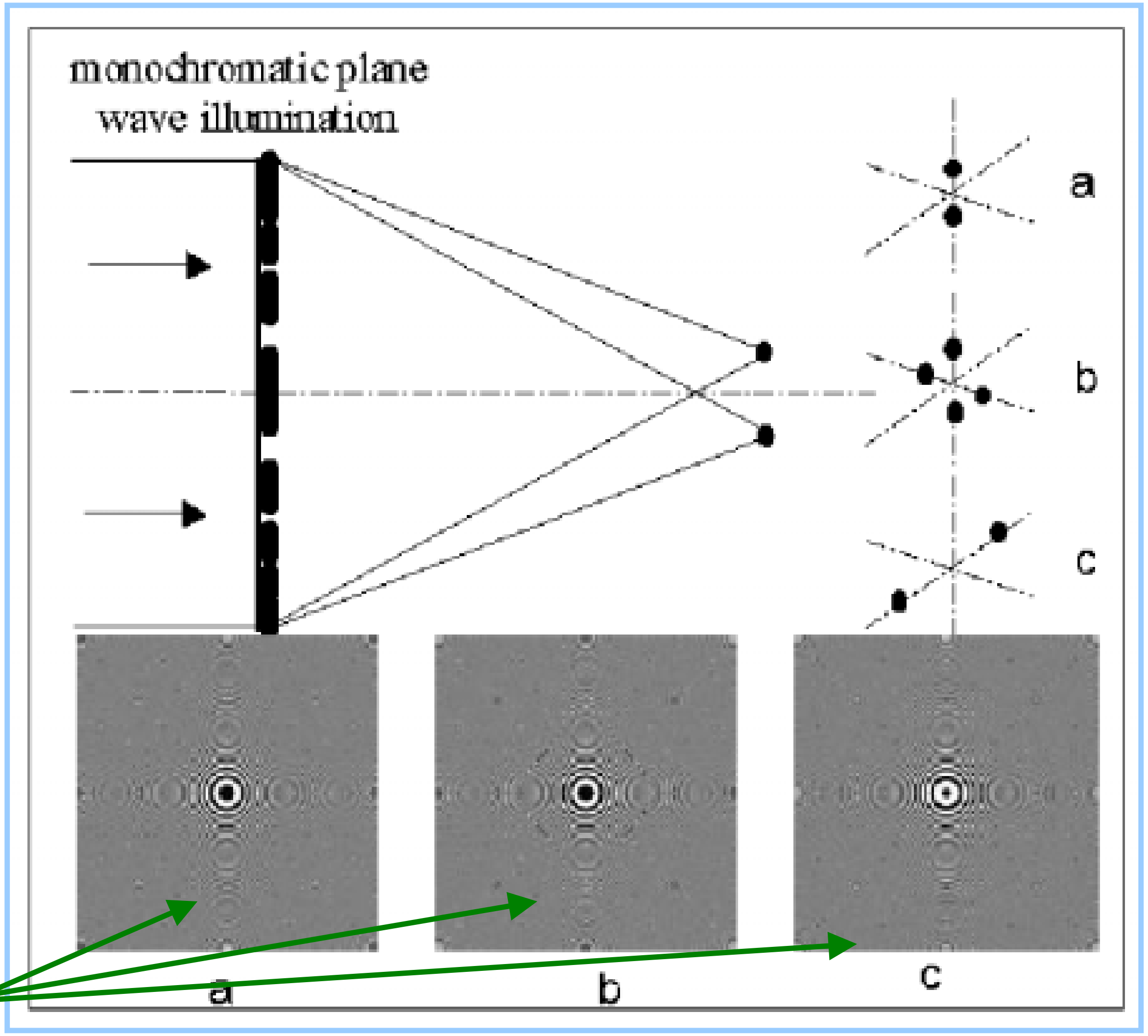

Multi-spot ZPs for DIC

Development of single, multi-spot zone plates by reconstruction of the hologram of a plane wave and several spherical waves (Lilit)

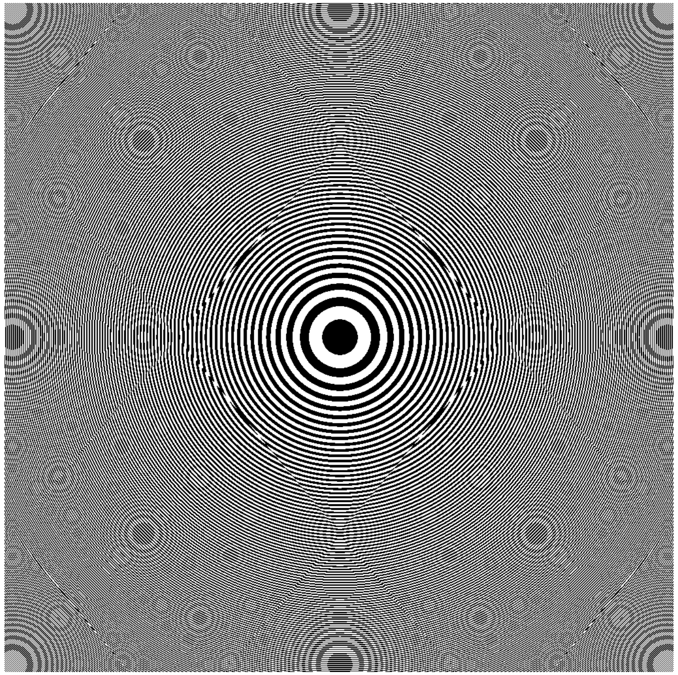

Calculated pattern of a 4 spot ZP

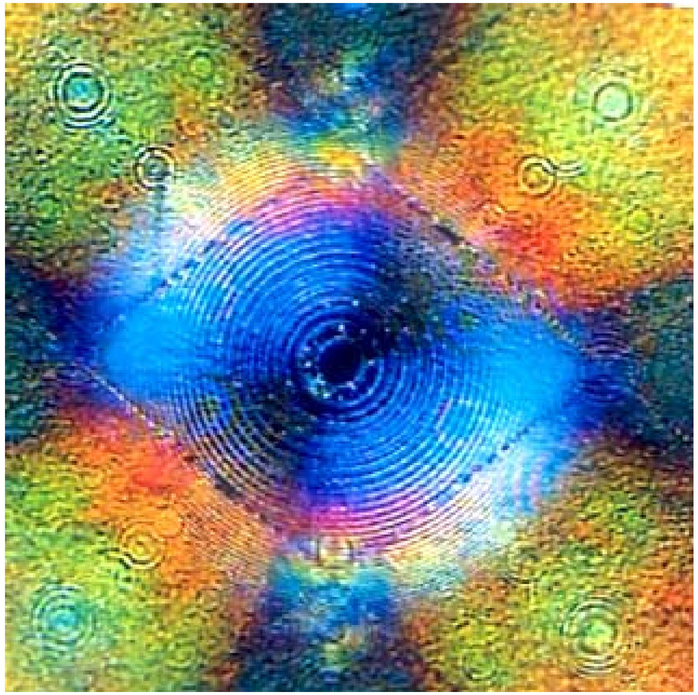

DIC visible light micrograph of 2-spot ZP

Multi-spot ZPs for DIC

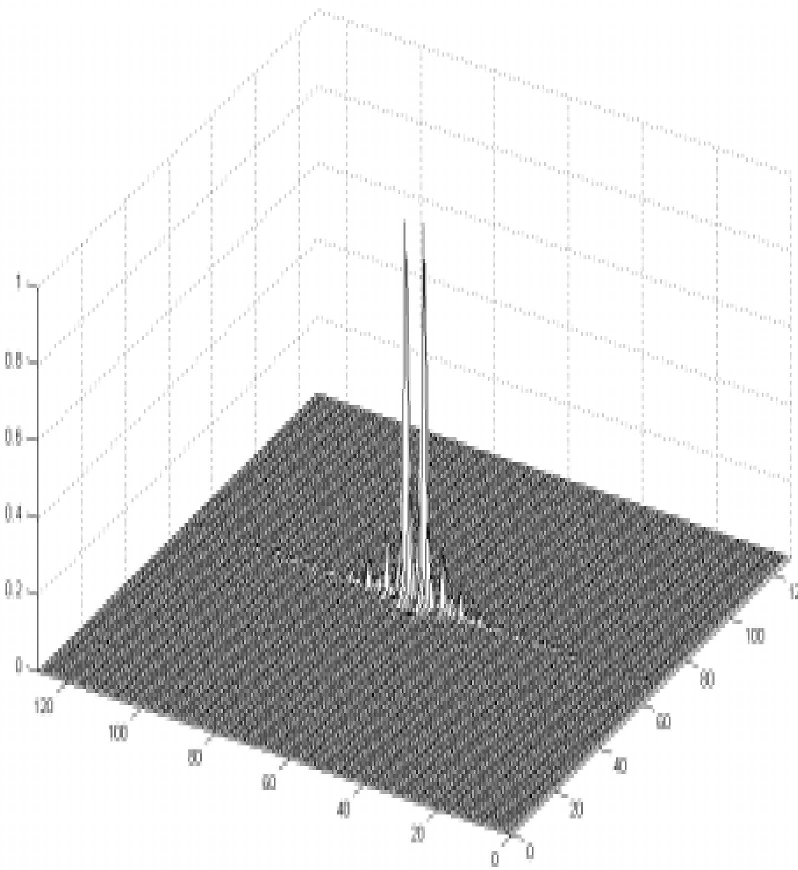

Simulation of 2-spot zone plate in / out focal plane

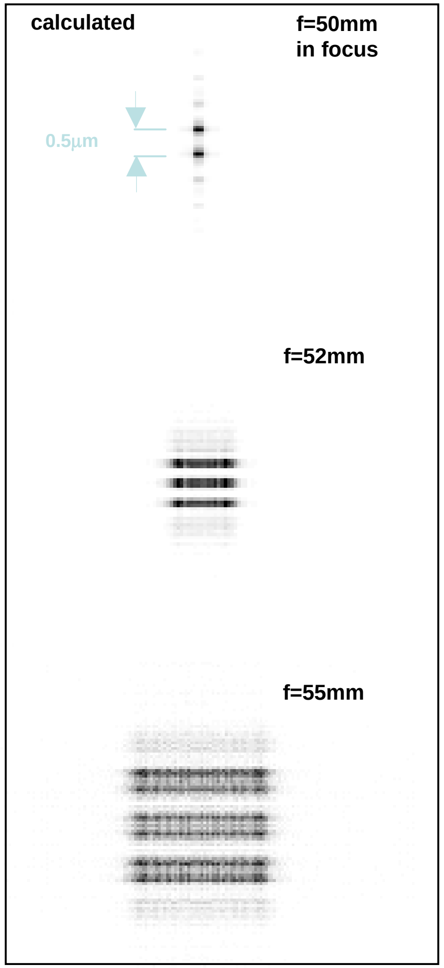

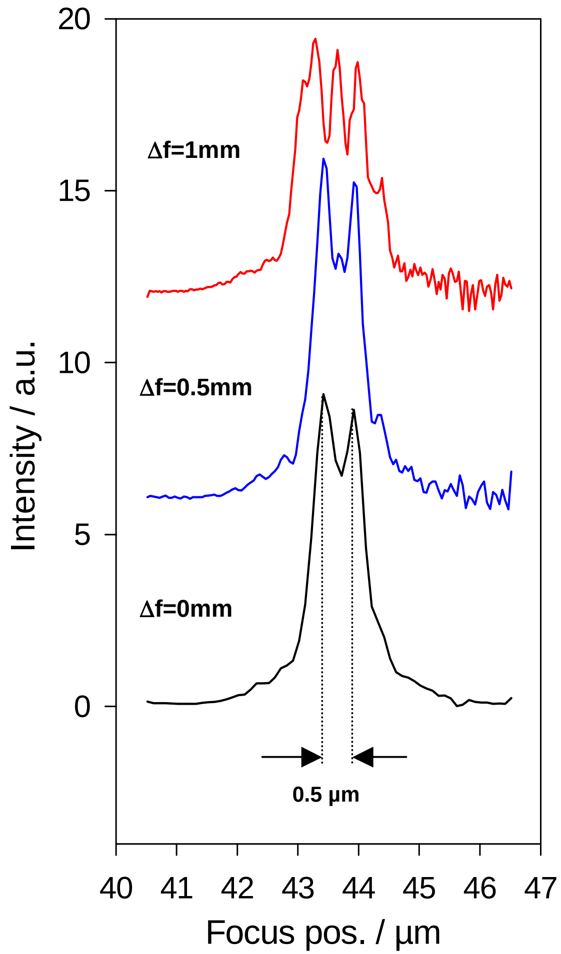

DIC with multi-spot ZPs (TXM)

X-ray images of 1 µm thick PMMA test objects

a, d: single zone plate

b, e: two confocal spots

c, f: two coaxial spots

ID21, TXM, λ = 0.31 nm

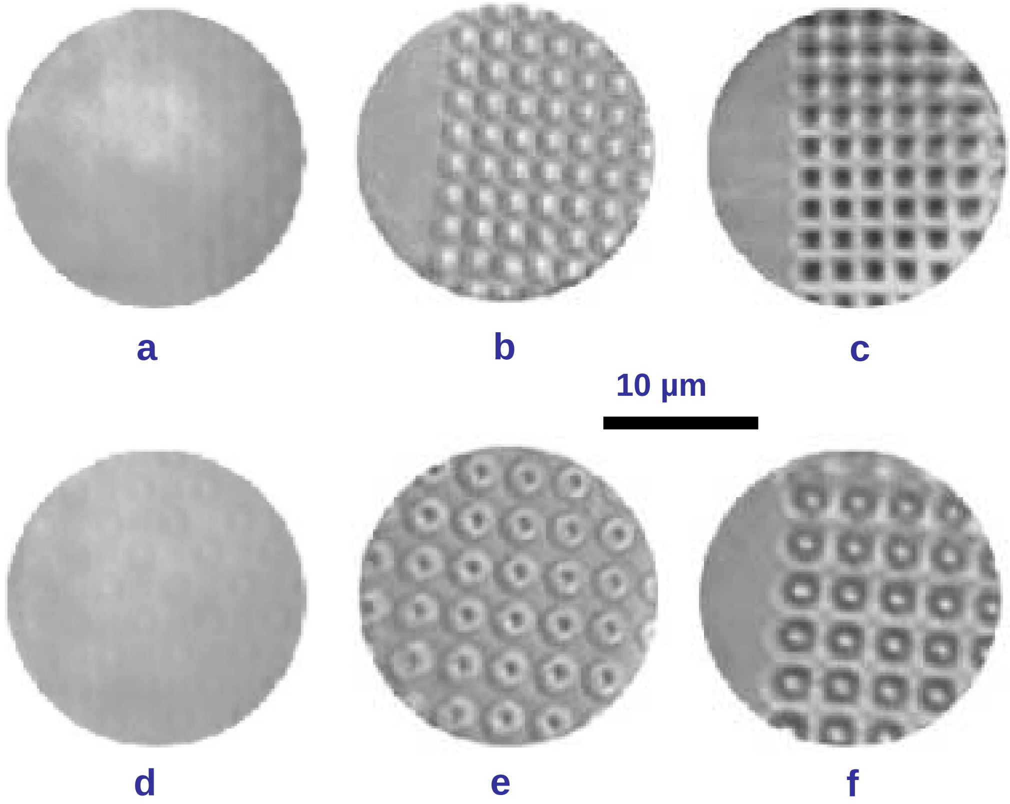

E. Di Fabrizio et al., subm. to Science

DIC with multi-spot ZPs (STXM)

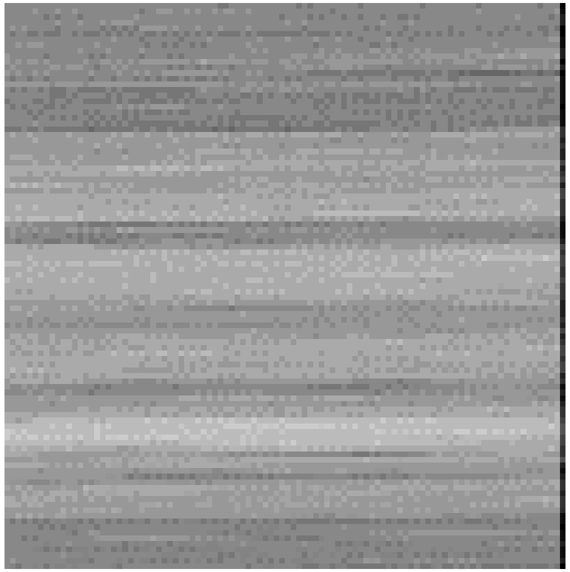

Brightfield (BF)

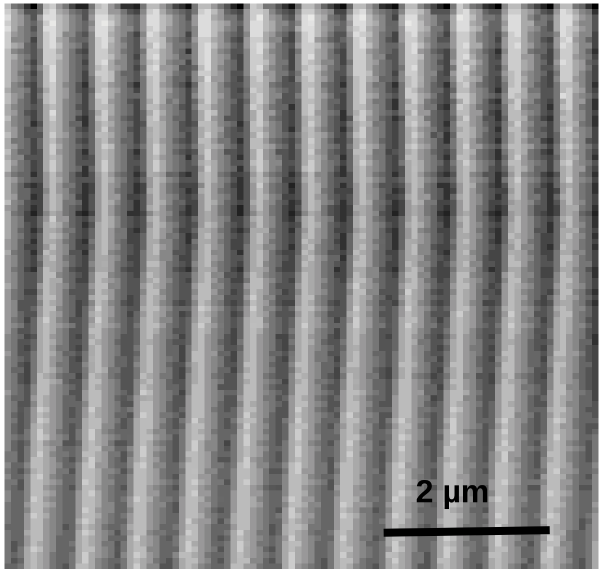

DIC

2 µm thick grating structures in PMMA

4 keV

200 x 200 px
40 ms/px dwell

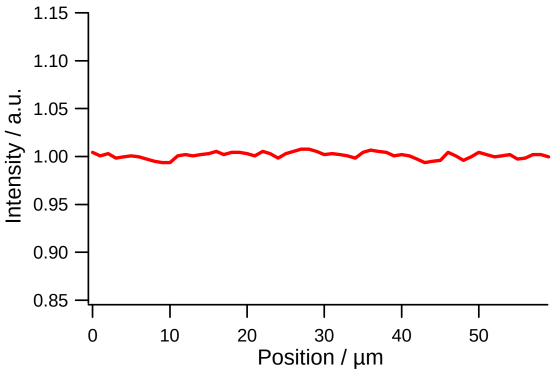

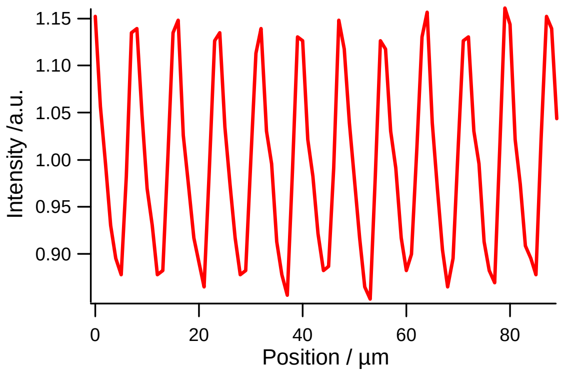

Contrast:

BF: 1 %
DIC: 25 %

Diffraction aperture based differential phase contrast

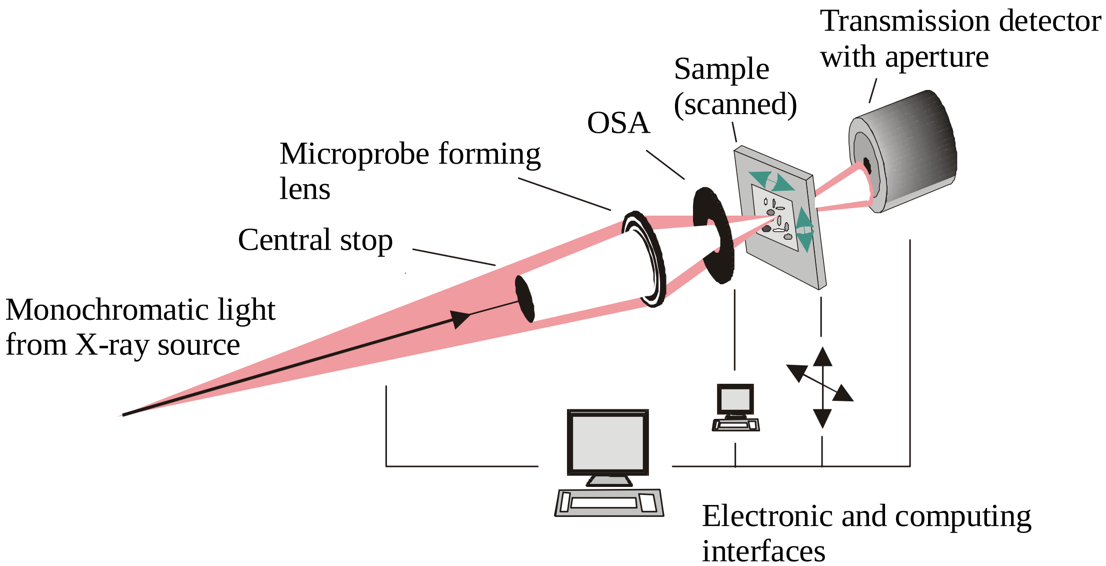

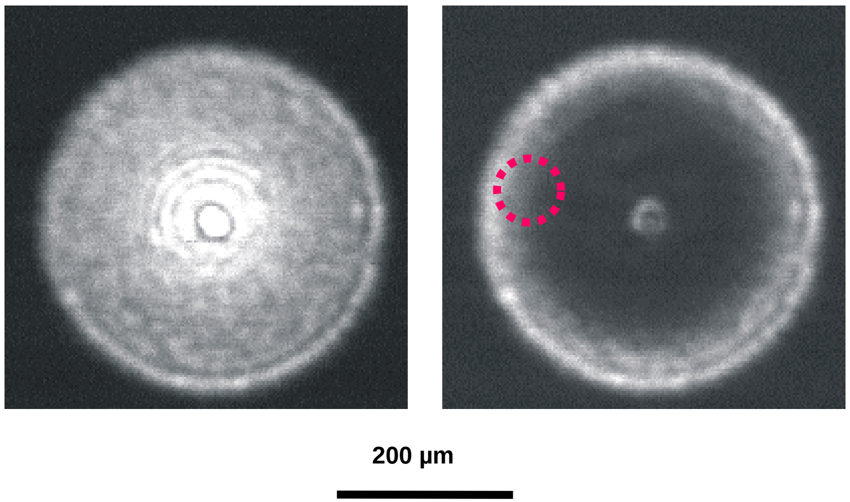

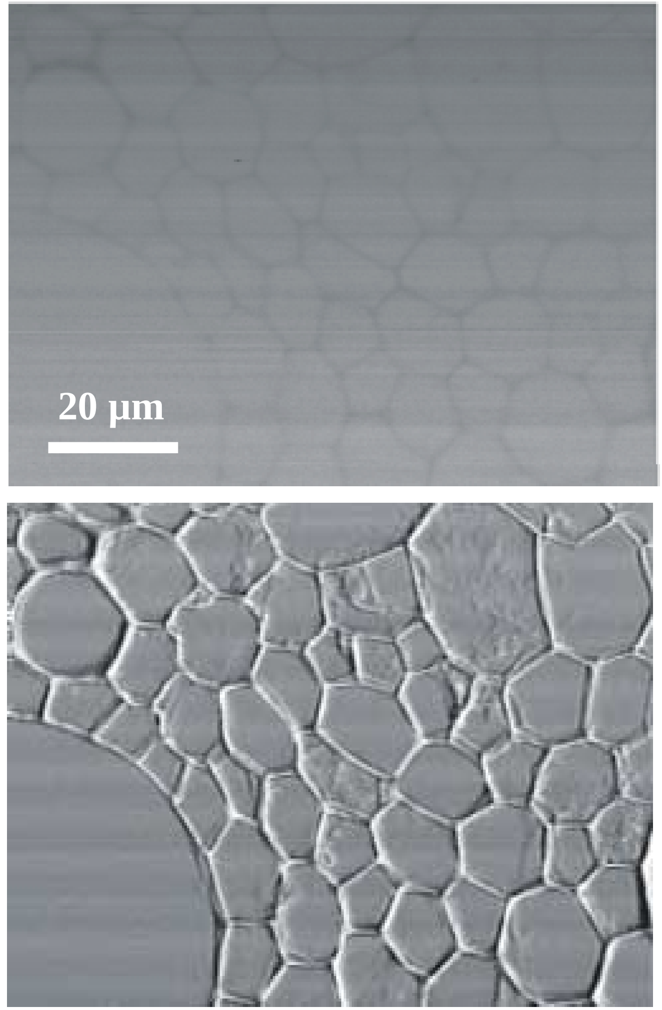

Principle: Differential phase contrast

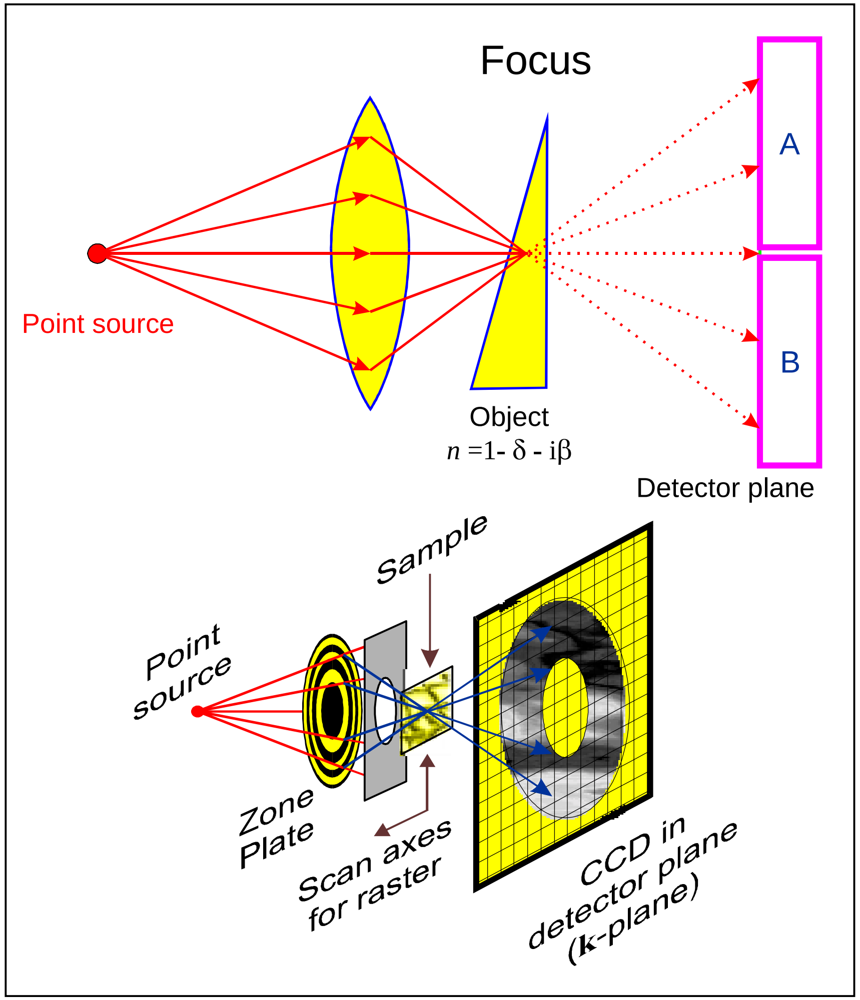

- **The detector can be split into several elements**
- **The sum signal gives the incoherent bright-field signal**
- **Anti-symmetric signal combinations relate to the *phase gradient* of the object transmittance.**

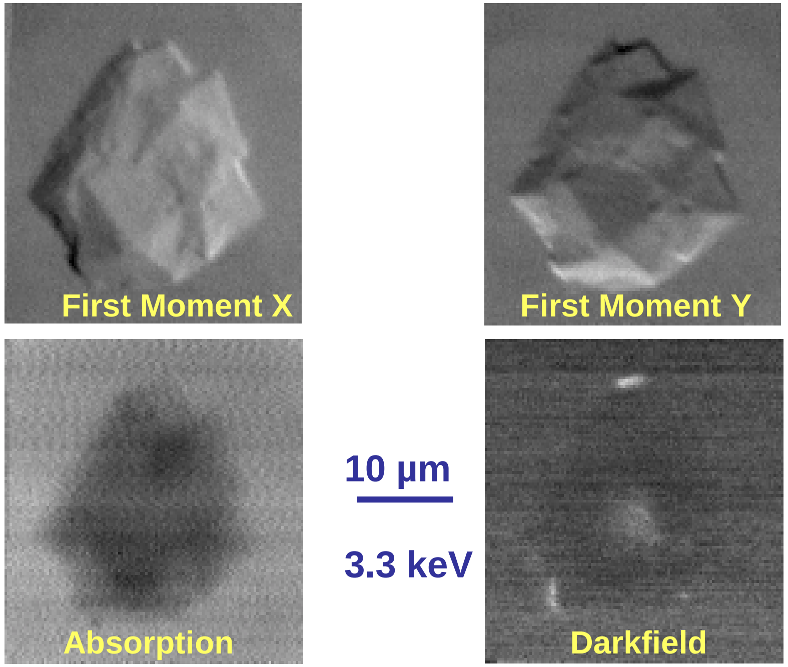

Chemical/ Magnetic contrast

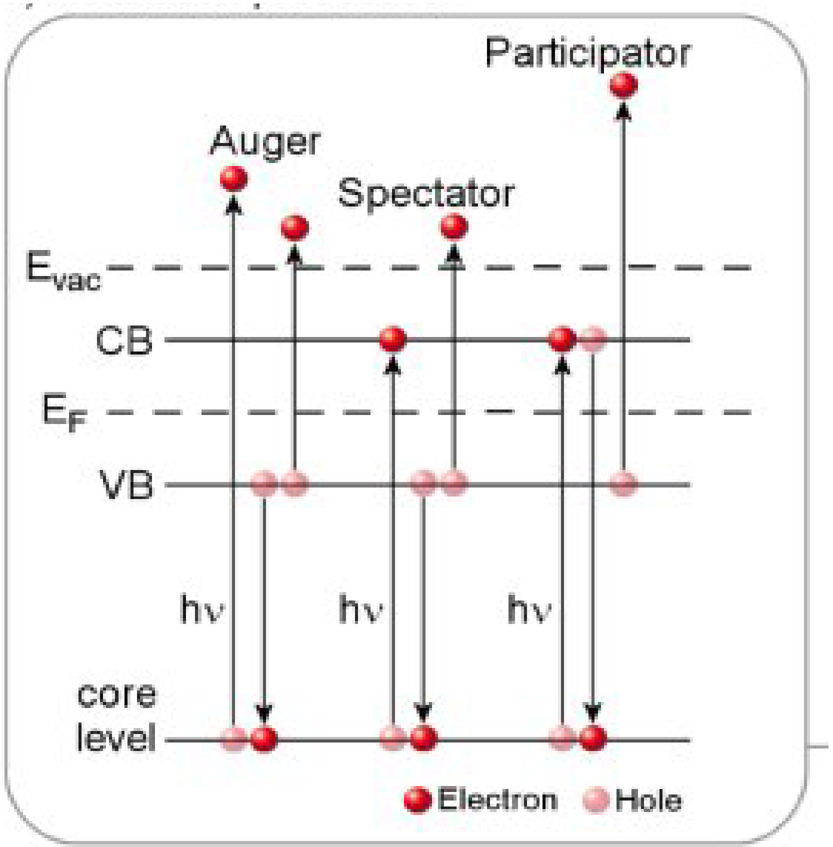

$$I \propto \exp(-\mu d) \;, \quad \mu \propto \frac{Z^z}{(h\nu)^3}$$

XANES = X-ray Absorption Near Edge Spectroscopy

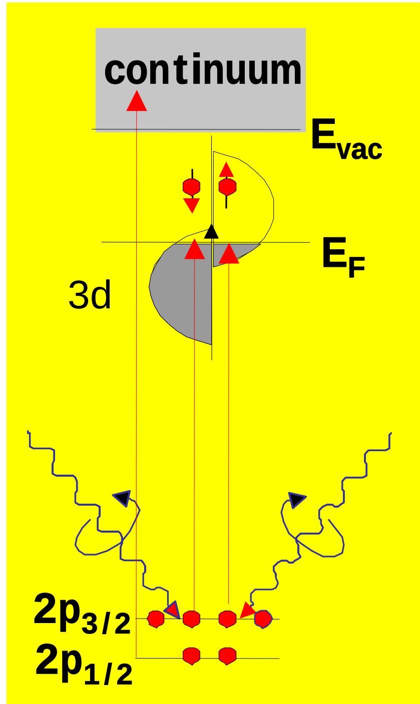

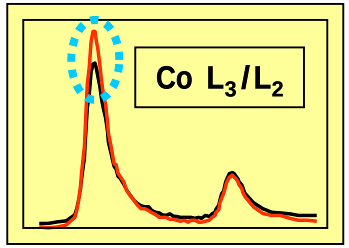

Resonances with unfilled states.

XANES: tuning on molecular orbitals
XMLD: imaging antiferromagnets,
XMCD: imaging ferromagnets

Chemical contrast

Outlining the lateral distribution of PS/ PMMA

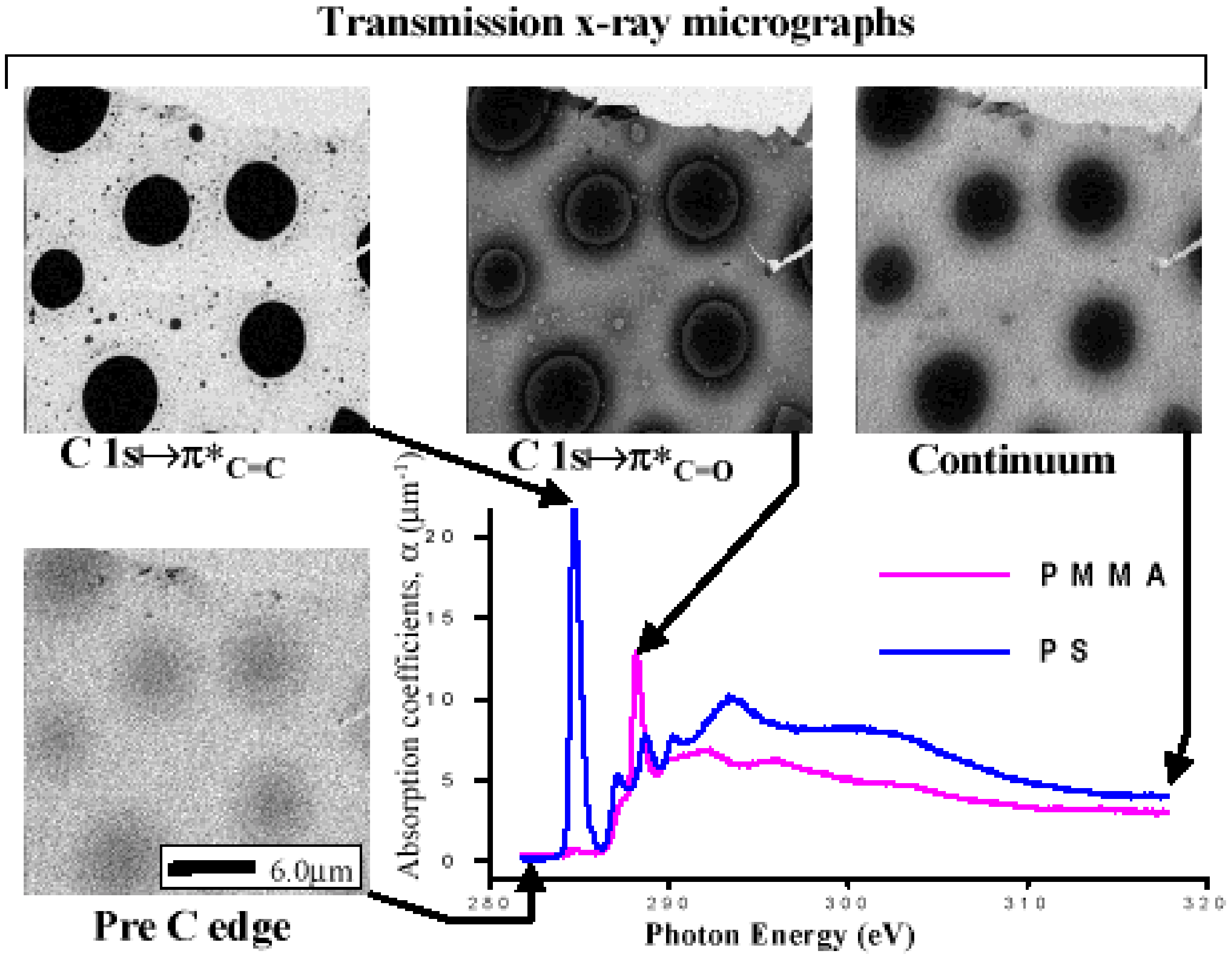

H. Ade, SUNY-SB STXM at the NSLS

Detector technologies for X-ray microscopy

- Basic properties
- Analog detectors
- Digital detectors (CCD, CMOS, photo diode, photo multiplier, drift detectors)
- Choosing the right detector

Human eye vs. electronic detectors

How does the human eye compare with electronic detectors?

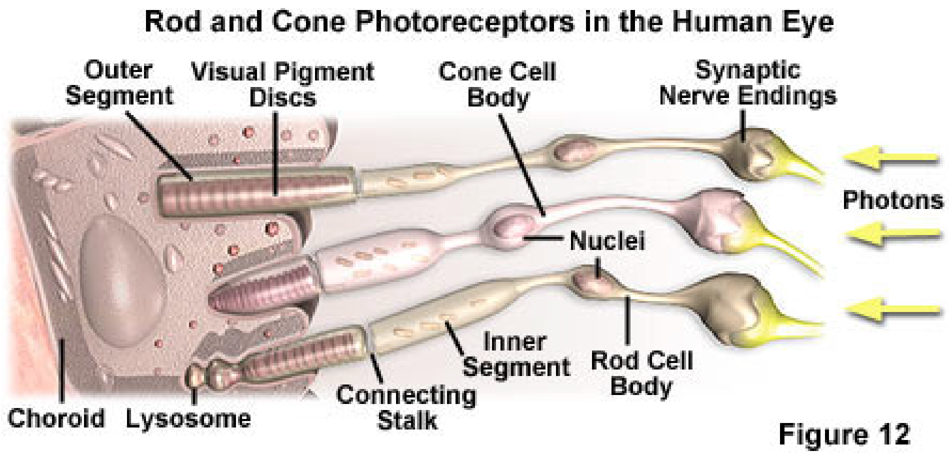

- Peak sensitivity is in the green (500 – 560 nm)
- Maximum quantum efficiency is 3 – 10 %
- Non-uniform spatial resolution due to not evenly distribution of cones
- Distance of cones > 1.5 μm, thus 5 – 6 μm on the retina
- Under achromatic illumination the dynamic is 50x (6 bits)
- Minimum detectable signal is about 100-150 photons at the pupil or 10 -15 ph at the retina
- Signal/noise limit is about 3:1

Scientific-grade camera:

- lower spatial resolution
- much higher quantum efficiency
- greater integration capability
- more uniformity
- better intrascene dynamic range
- comparable or higher signal/noise
- sensitive to X-rays

Basics: Quantum efficiency

For a detector, the ratio of induced current to incident flux. Often measured in electrons per photon (dimensionless) or amps/watt.

Mean energy to generate an electron-hole pair in Si-based detectors:

E = 3.7 eV

Mean number of electrons per incident photon:

$$n_{\max} = \frac{h\nu}{3.7eV}$$

Energy related quantum efficiency (QY) is the ratio of measured electrons per incident photon to maximum electrons per incident photon

$$QY = \frac{n_{\det}}{n_{\max}} = \frac{n_{\det} \cdot 3.7eV}{h\nu}$$

Basics: CCD dynamic range

The dynamic range (DR) of a CCD is typically specified as the maximum achievable signal divided by the camera noise, where the signal strength is determined by the full-well capacity and noise is the sum of dark and read noises

Full well capacity N_{sat}: The number of electrons that each pixel of a charge-coupled device can hold without overflowing and causing blooming.

N_{noise}: The total value of the read and dark noise

$$DR = 20 \cdot Log(\frac{N_{sat}}{N_{Noise}})$$

or

$$DR = \frac{N_{sat}}{N_{Noise}} \approx \frac{1000 \cdot d_{ph}}{N_{Noise}}$$

Example: CCD with 6.7µm pixel size ⇨ N_{sat} = *44900 e/px*
Read noise of N_{Noise} = *500 e/px*
⇨ DR = 90 or 39db

Scientific-grade CCDs: DR = 50000 or 94db

Detectors: Avalanche photodiode

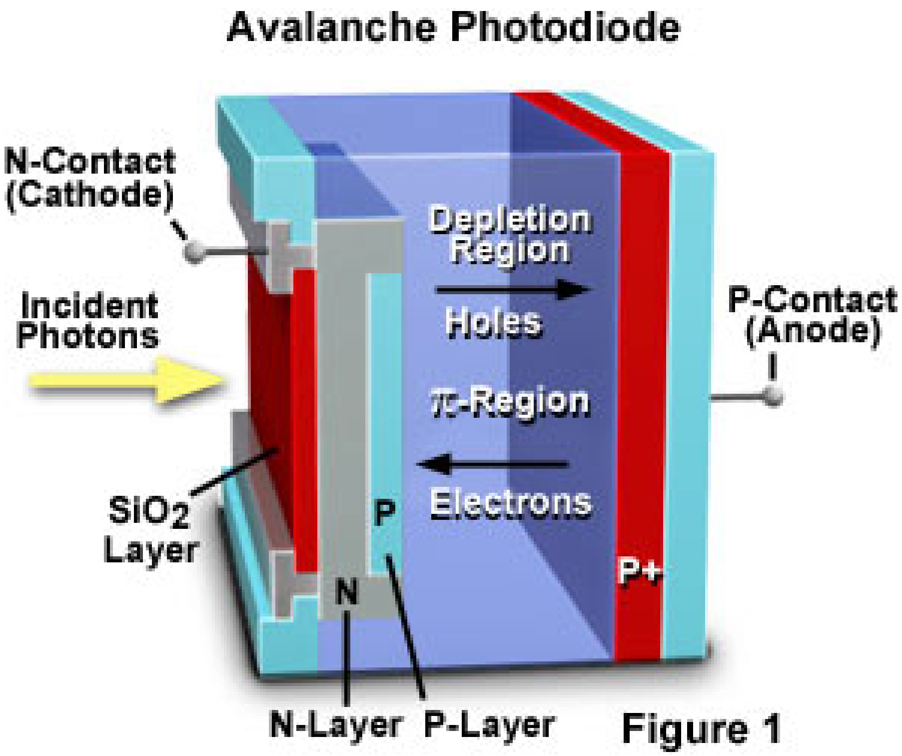

Silicon-based semiconductor containing a positively doped p-region and a negatively doped n-region sandwiching an area of neutral charge termed depletion zone

- **Generation of electron-hole pairs from an energetic electron that creates an "avalanche" of electrons in the substrate (high bias voltage)**
- **Design is similar to p-i-n diodes, however the depletion layer is relatively thin**
- **Compact and immun to magnetic fields, require low currents, are difficult to overload**
- **High quantum efficiency up to 90%**

Detectors: Photomultipliers

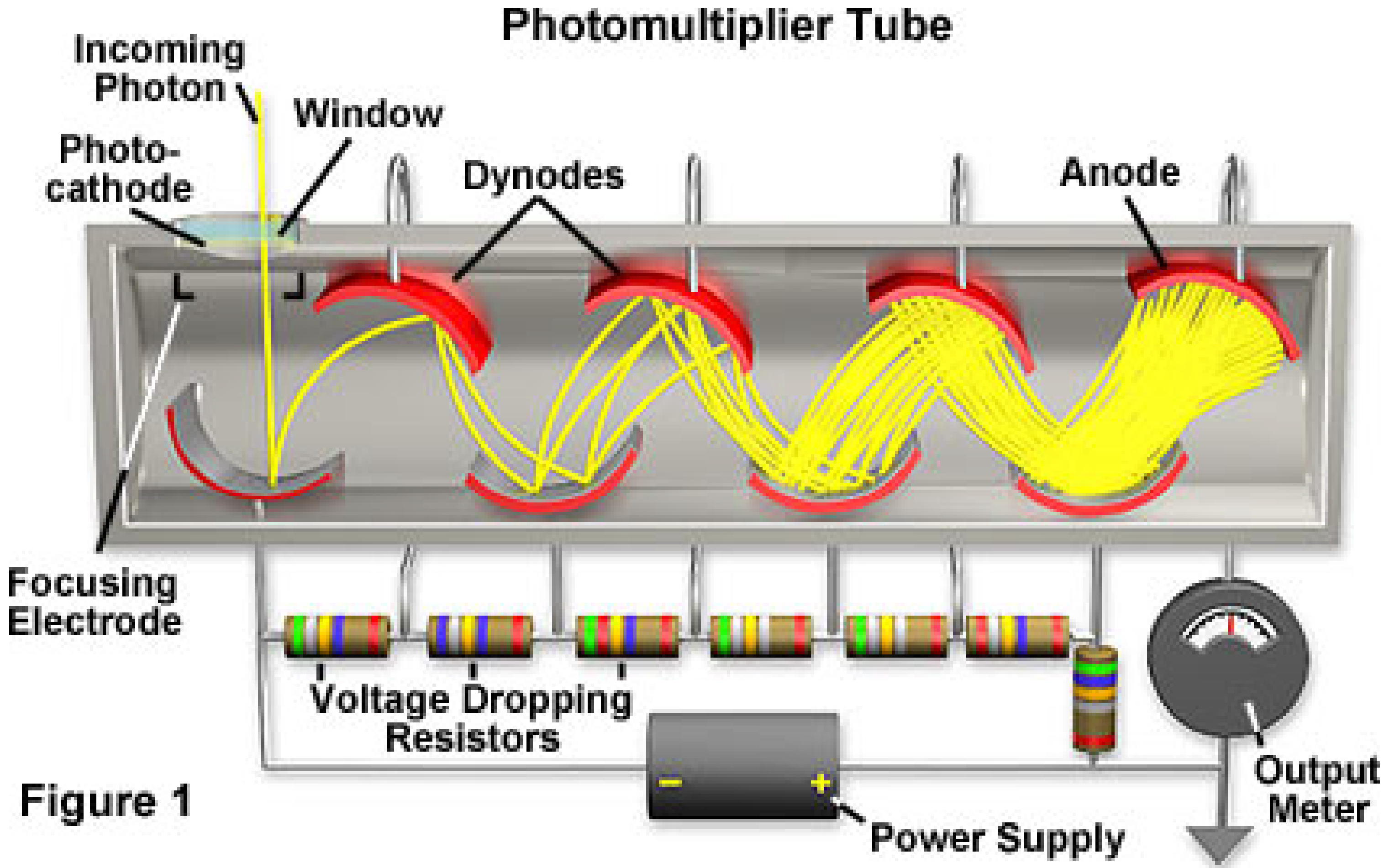

Detectors: Charge coupled devices (CCDs)

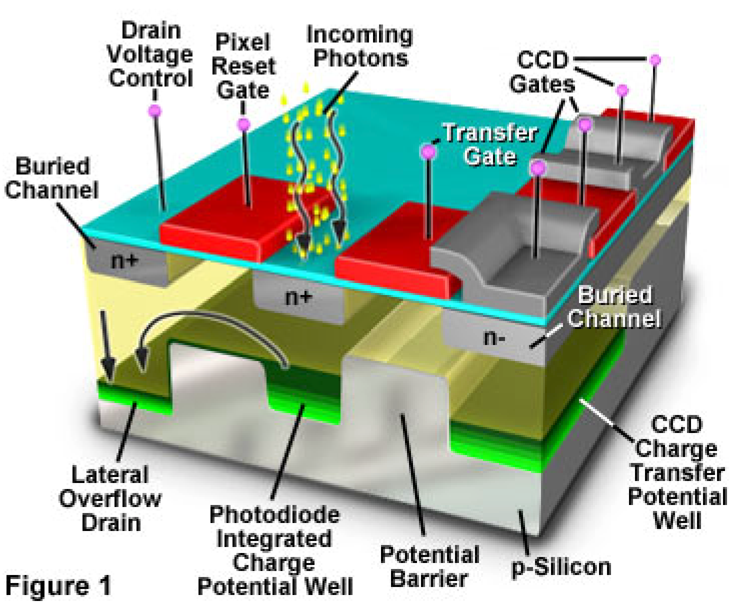

Figure 1

Silicon-based integrated circuits consisting of a dense matrix of photodiodes that operate by converting light energy (photons) into electric charge that are stored in potential wells and are subsequently transferred across registers and output to an amplifier

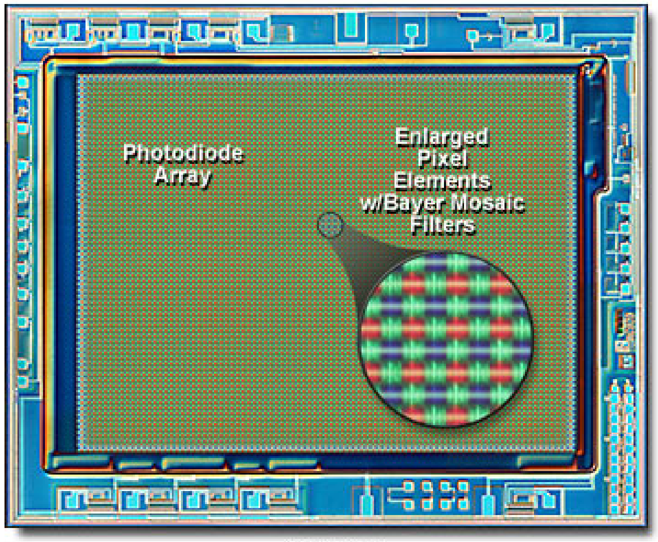

Figure 2

- **Invented in the late 60's at Bell Labs**
- **Initially conceived as idea for new type of memory circuit for computers**
- **Leading candidate for all-purpose imaging detector**

Detectors: Charge coupled devices (CCDs)

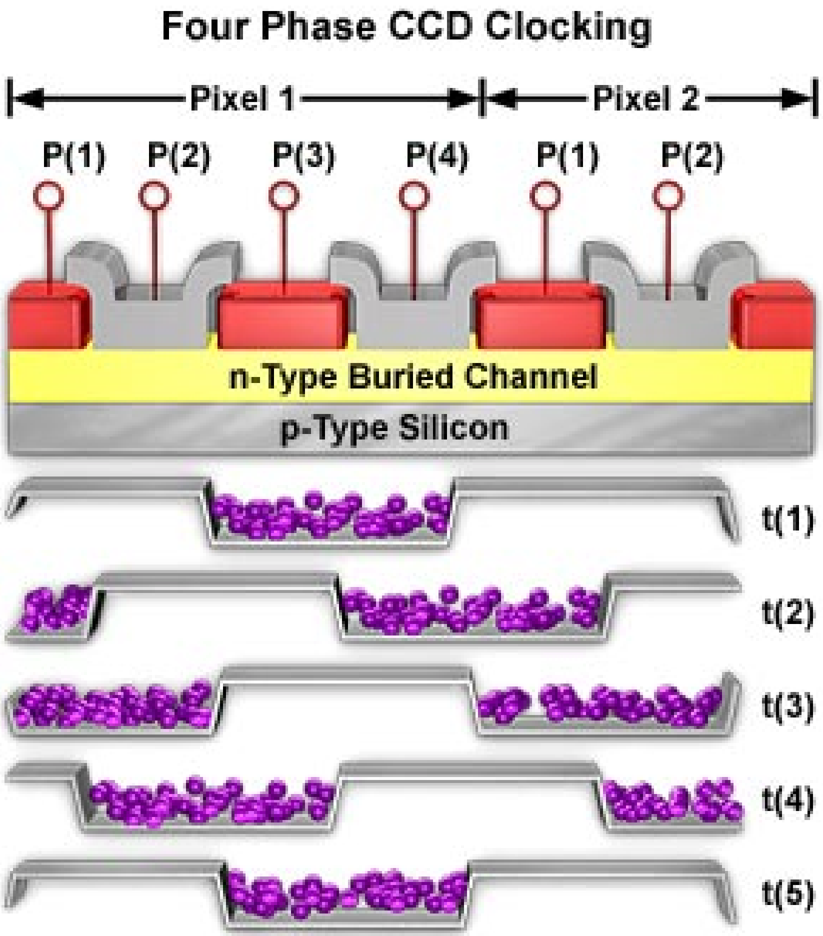

Figure 1

PIXEL = PHOTODIODE

Silicon-based integrated circuits consisting of a dense matrix of photodiodes that operate by converting light energy (photons) into electric charge that are stored in potential wells and are subsequently transferred across registers and output to an amplifier

t(1): Voltage at gate P(1) and P(2) low, P(3) and P(4) held high

t(2): P(1) and P(3) change polarity

t(3): P(2) on both pixels switches from low to high, P(4) on pixel 1 switches from high to low

t(4): One cycle of charge transfer completed

Detectors: MOS capacitor

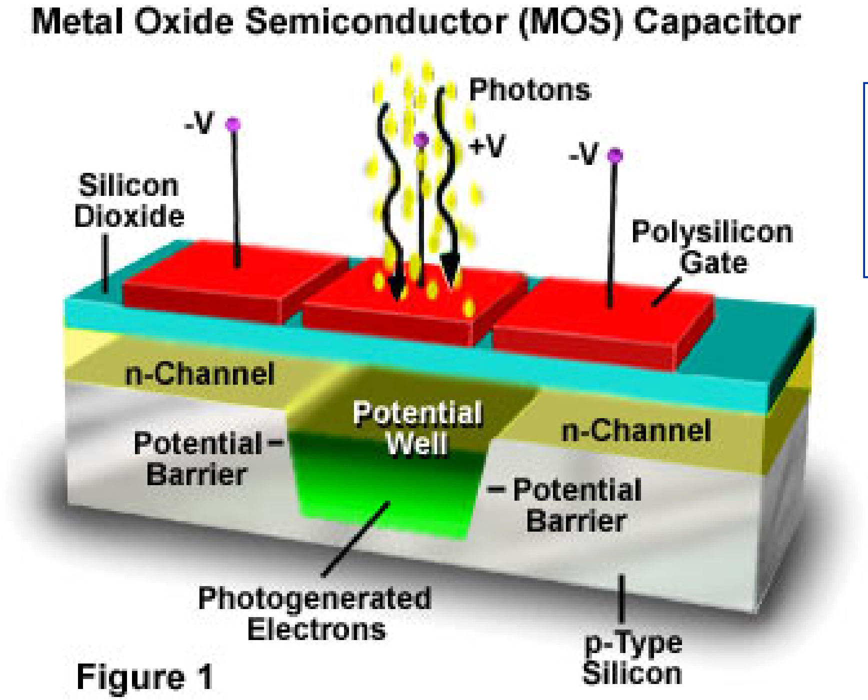

Figure 1

At the heart of all CCDs is the light sensitive *metal oxide semiconductor (MOS)* capacitor

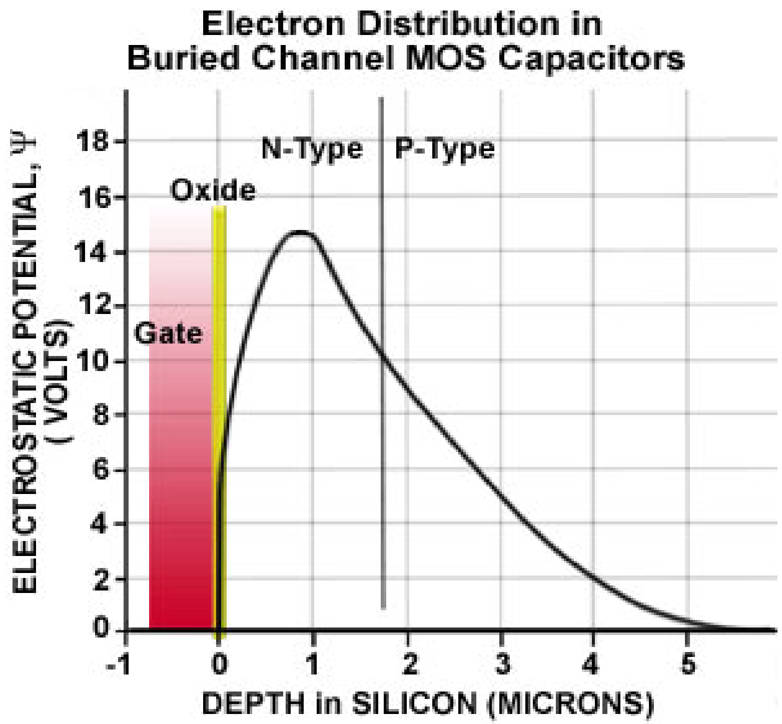

Figure 2

Application of voltage will flatten the electrostatic potential curve at the peak

Detectors: CMOS technology

Complementary Metal Oxide Semiconductor

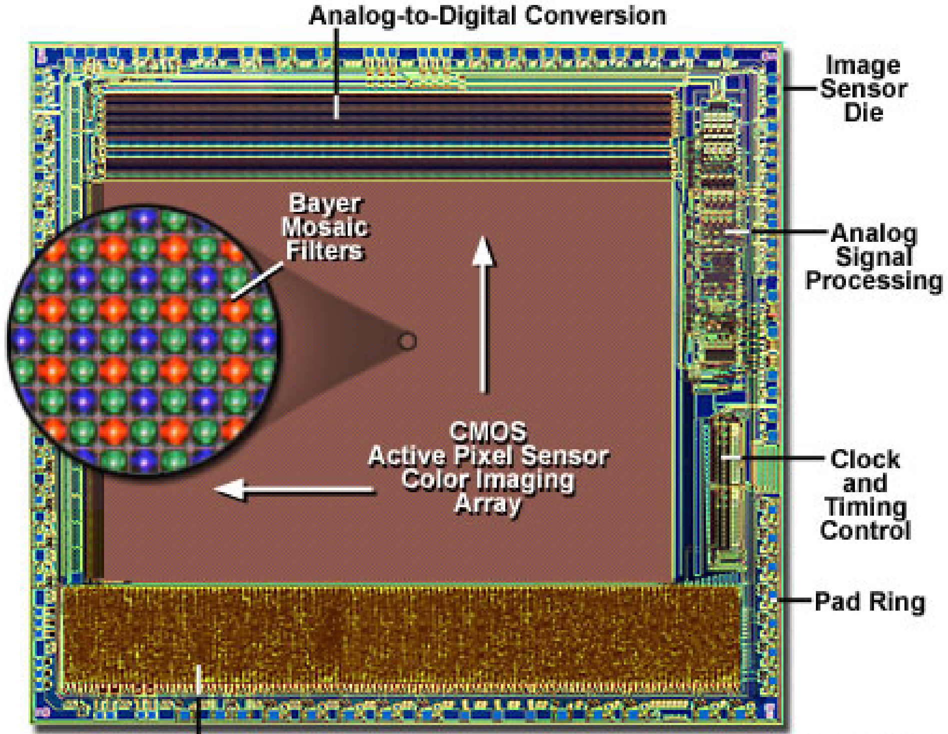

Figure 1

Light sensing similar to CCDs (photo-electric effect)

- **Lower power consumption**
- **Smaller pixel sizes**
- **Reduced noise**
- **More capable on-board image processing algorithms**
- **Larger imaging arrays**

Fillfactor: 30 – 80 % of pixel area

Bayer Color Filter Mosaic Array and Underlying Photodiodes

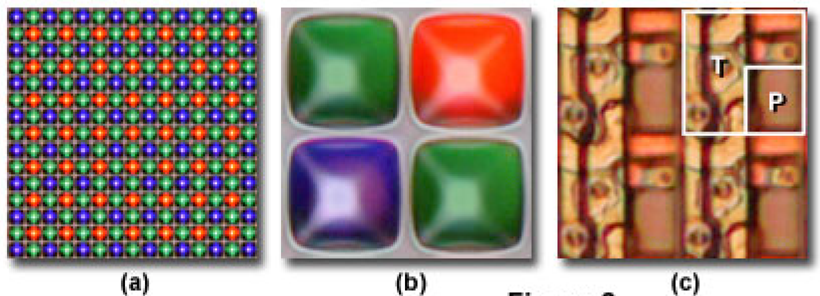

Figure 2

Detectors: CMOS technology

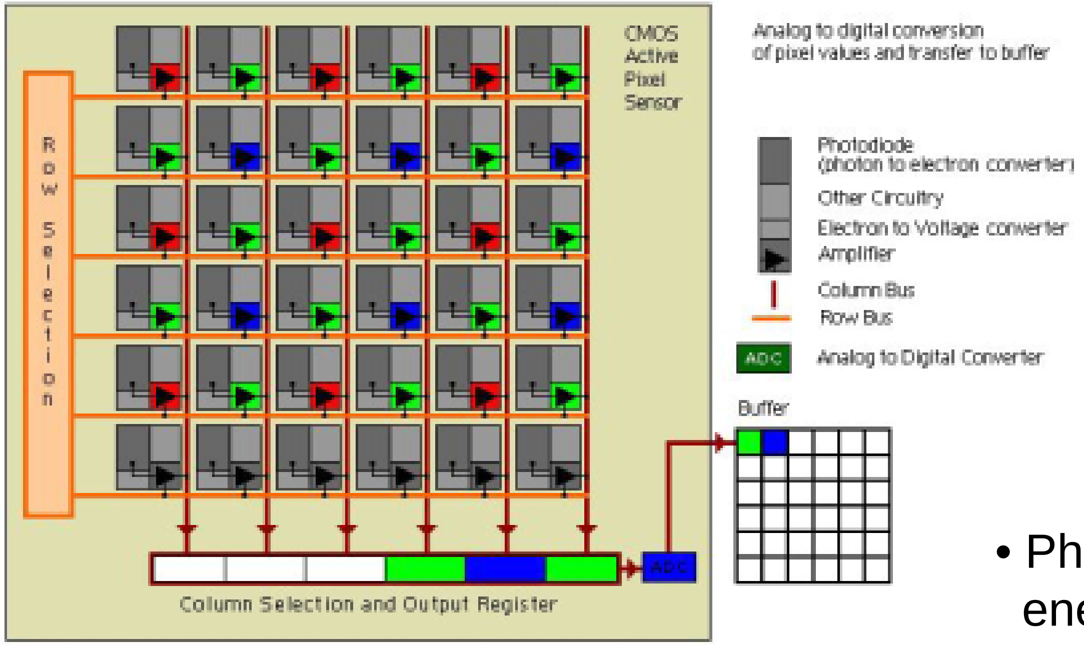

- Photodiode convert energy into electrical discharge
- Electrical discharge is converted amplified into voltage
- Pixel values are sequenced (multiplexed) and processed by the ADC
- Pixel values are buffered

Energy dispersive detectors: SDDs

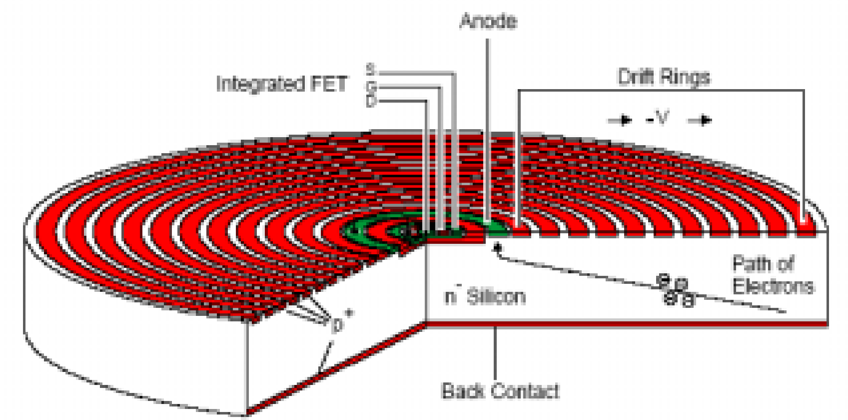

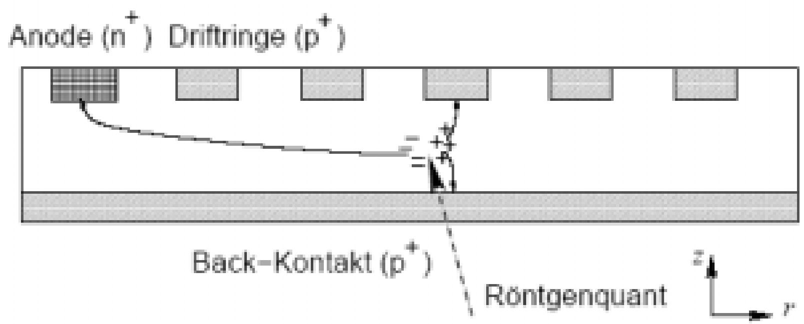

- **Principle of sideward depletion**
- **Electric field transports e^- to the anode with integrated FET**

<u>Energy dispersion:</u>

$$n_{\max} = \frac{h\nu}{3.7eV}$$

Number of electrons is counted

References

J. Kirz, C. Jacobsen, and M. Howells, “Soft X-ray microscopes and their biological applications” Q. Rev. Biophys. 28(1), 33-130 (1995)

D. Attwood “*Soft X-rays and Extreme Ultraviolet Radiation”,* Cambridge Press, Cambridge, UK (1999)

G. Schmahl et al., “Phase contrast studies of Hydrated Specimens with the X-ray microscoe at BESSY, in: Aristov et al. (eds.), X-ray microscopy IV, Bogorodski Pechatnik Publishing, Chernologovka, Moscow Region (1994)

G. Schneide, “*X-ray microscopy: methods and perspectives”,* Anal. Bioanal. Chem. 376(5), 558-561 (2003)

D. Weiss et al.: “*Tomographic imaging of biological specimens with the cryo transmission X-ray microscope”,* Nucl. Instrum. Meth. A 476, 1308-1311 (2001)

G. Schneider, “*Cryo X-ray microscopy with high spatial resolution in amplitude and phase contrast,* Ultramicroscopy 75(2), 85-104 (1998)

W. Meyer-Ilse, T. Warwick, and D. Attwood (eds.), AIP Conf Proc **507** (1999)

M. Feser et al.; *“Scanning transmission X-ray microscopy with a segmented detedtor”,* J. Phys. IV 1 (2002)

F. Polack, D. Joyeux, J. Svaloš, and D. Phalippou
“Applications of wavefront division interferometers in soft x rays”, Rev.Sci. Instrum. **66**, 2180 (1995);

T. Wilhein, B. Kaulich, and J. Susini
“*Two zone plate interference contrast microsopy at 4 keV photon energy”,* Opt. Commun. **193**, 19-26 (2001)

T. Wilhein, B. Kaulich, E. Di Fabrizio, S. Cabrini, F. Romanato, and J. Susini
”Differential interference contrast X-ray microscopy with submicron resolution”
Appl. Phys. Lett. **78**, 2079-2081 (2001)

B. Kaulich, T. Wilhein, E. Di Fabrizio, F. Romanato, M. Altissimo, S. Cabrini, B. Fayard, J. Susini
“Differential interference contrast x-ray microscopy with twin zone plates“, JOSA A **19** (4), 797-806 (2002)

Practical course:

1. **Introduction to properties of digital images**
   Digital image formats, sampling and quantization, image resolution, Shannon's sampling theorem, color/ grayscale histograms

2. **Digital image processing**
   Pre-processing evaluation of raw images, flat-field correction and background correction, digital image histogram adjustment, convolution kernels and filters for image processing, Fourier transforms